Intended for
The Danish EPA

Document type
Report

Date
May 2022

Hydrological model for Saldanha Bay

HYDROLOGICAL MODEL FOR SALDANHA BAY, SOUTH AFRICA
MODEL REPORT

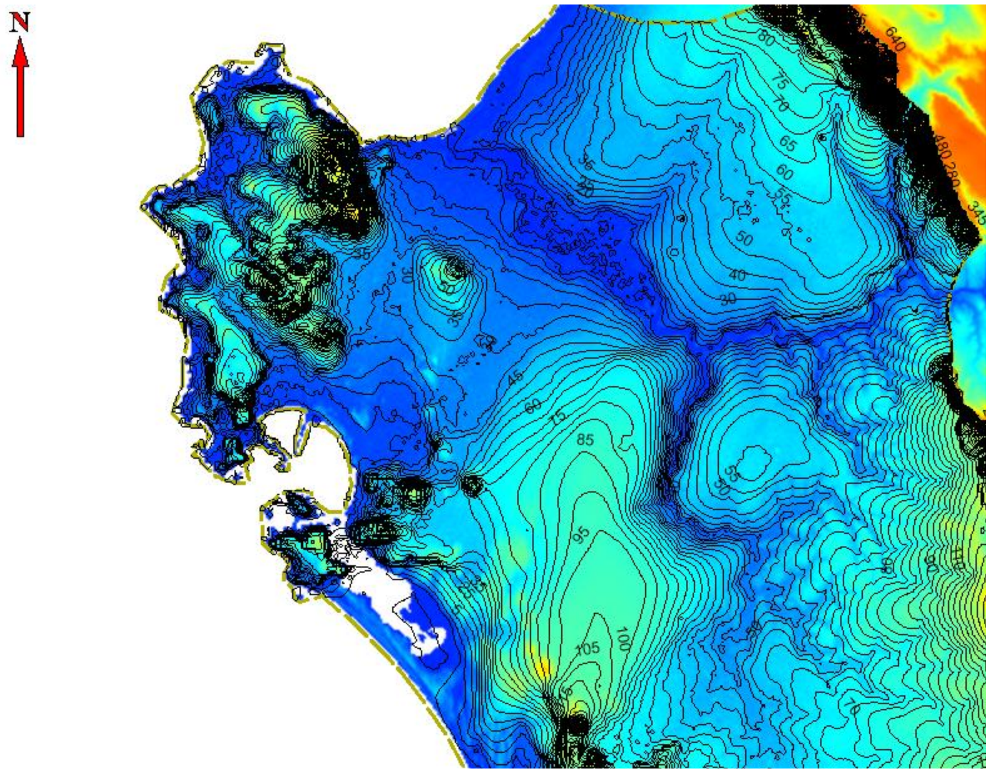

HYDROLOGICAL MODEL FOR SALDANHA BAY, SOUTH AFRICA
MODEL REPORT

Project name	**Saldanha Bay -Wellfield management System (WfMS)**
Project no.	**1320044223**
Recipient	**Danish EPA**
Document type	**Report**
Version	**[01]**
Date	**08/04/2020**
Prepared by	**Jan Kürstein**
Checked by	**Anker Lajer Højberg**
Approved by	**Jan Kürstein**
Description	**Hydrological model rapport for Saldanha Bay**
[Optional 1]	**Hydrological model for Saldanha Bay**

Ramboll
Hannemanns Allé 53
DK-2300 Copenhagen S
Denmark

T +45 5161 1000
https://ramboll.com

Rambøll Danmark A/S
DK reg.no. 35128417

Member of FRI

CONTENTS: A DESCRIPTION OF THE HYDROLOGICAL MODEL FOR SALDANHA BAY

1. MODEL SYSTEM

The model system used is MIKE SHE /1/. MIKE SHE covers the water cycle on land, as shown on Figure 1 and integrates different packages describing the different parts of the land based freshwater cycle:

-the root zone, EP package
-overland flow, OL package
-the unsaturated zone, UZ package
-the saturated zone, SZ package
-flow in rivers and lakes, MIKE 11 (or MIKE HYDRO RIVER)

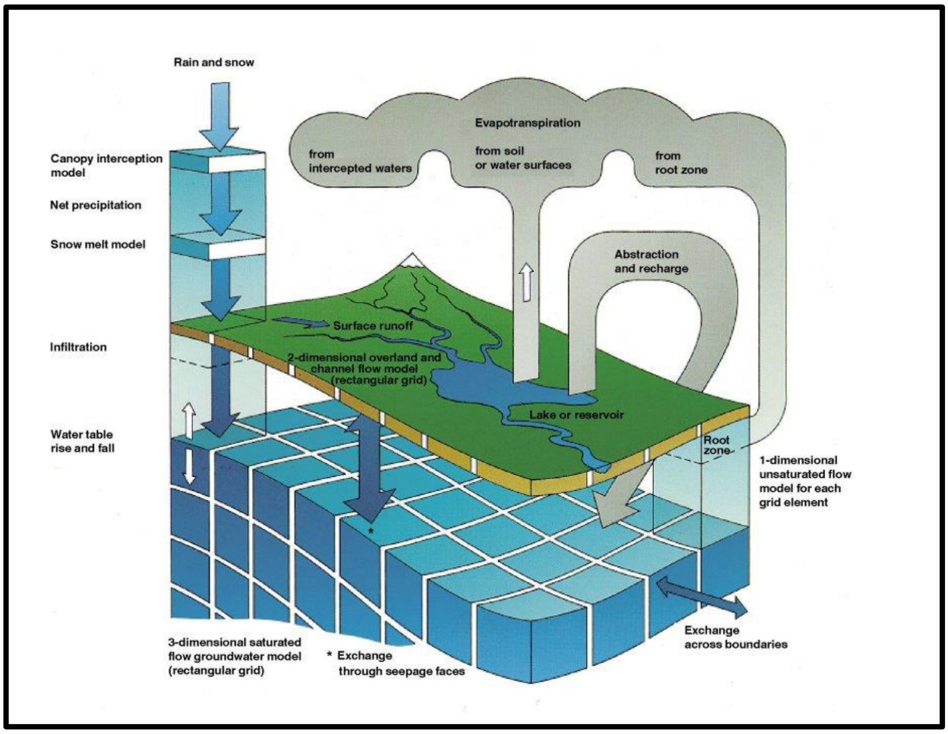

Figure 1 The model system – MIKE SHE

Using the integrated approach in MIKE SHE the net precipitation is calculated as a part of the modelling process, so it is not necessary to calculate it prior to the modelling. This is very suitable in transient modelling and semi-arid climates with high evaporation and changes between wet and dry seasons.

2. SALDANHA BAY

2.1 Hydrological model area

The model area is within the Saldanha Bay Local Municipality and shown in Figure 2. The boundary of the model area follows mostly robust hydrological boundaries as the ocean and topographic heights. The only exception is the northern boundary and where Berg River enters the model area at the eastern boundary. The northern boundary is perpendicular to the coast following the assumed groundwater flow direction in this area with no significant groundwater flow across this line. Where Berg River enters the area, there is a significant inflow of surface water in the river and probably a minor inflow of groundwater. The western boundary consists of the Atlantic Ocean.

The model area is 5135 km^2. The location of the model area is north of Cape Town as shown on Figure 3

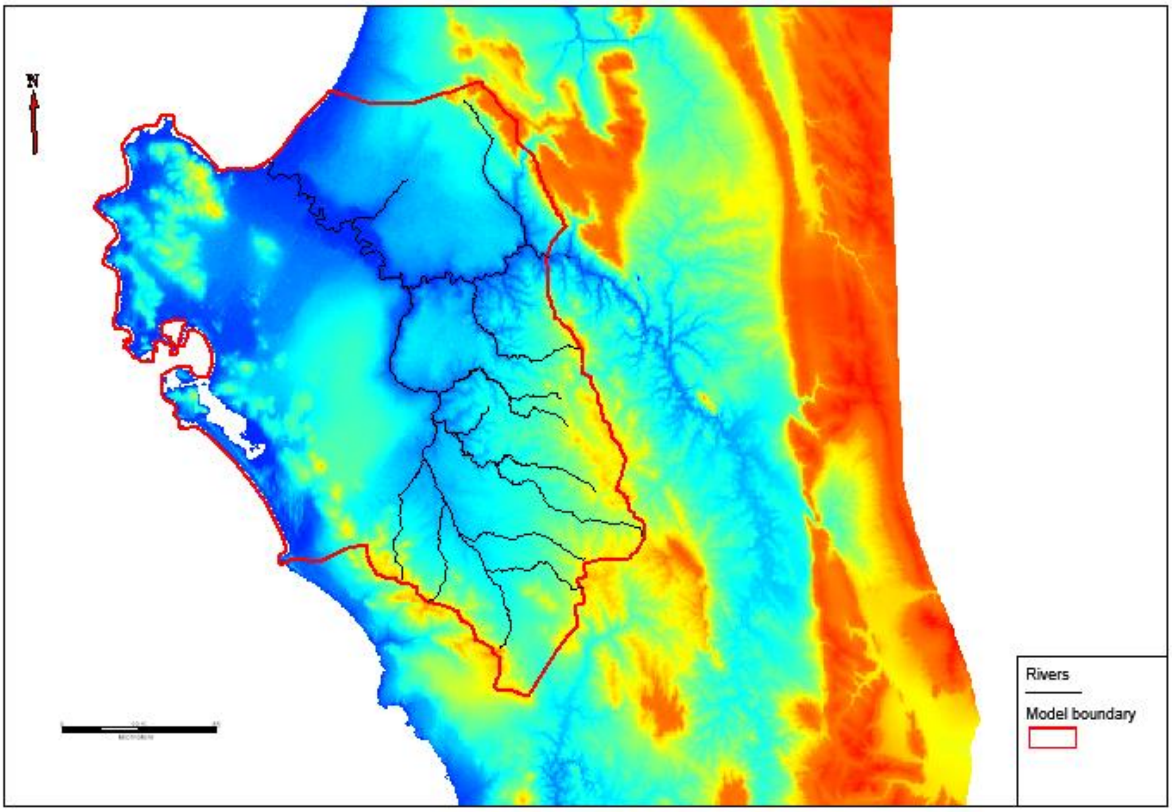

Figure 2 Model Area

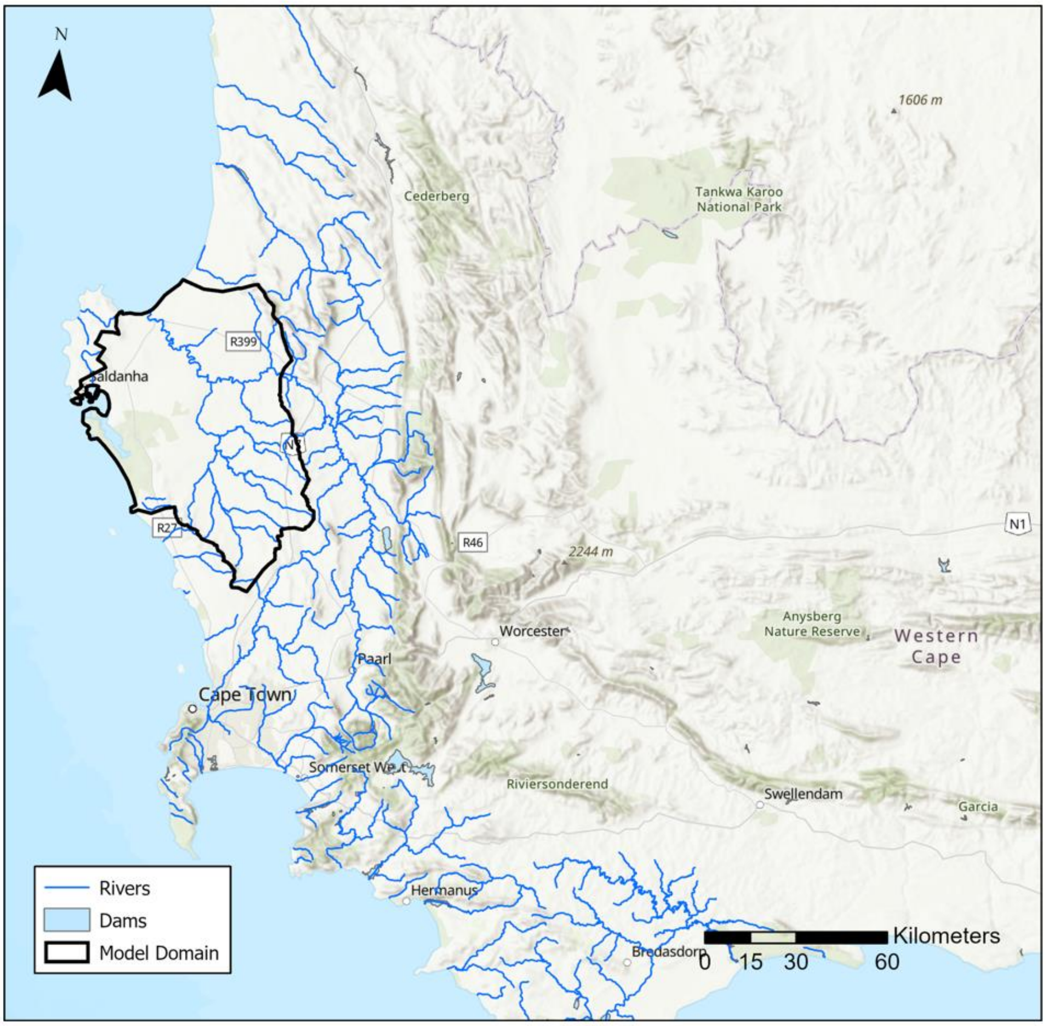

Figure 3 Rivers and dams in the area

2.2 Current water supply system

The current water supply system in Saldanha Bay Local Municipality is primarily based on surface water being transported in a pipeline from surface water dams located in the mountains around Franschhoek's in the mountains west of Cape Town opposite the Cape Flats. To increase drought resilience, more groundwater is planned to be implemented in the bulk water supply. There has been established two well fields in the area, the Langebaan Wellfield and Hopefield Wellfield, respectively. The locations of the well fields are shown in Figure 4. Langebaan wellfield was used during the draught period around 2018 and has an active permit. However, the wellfield is presently not operated continuously, but only active part of the time. A license has been applied for at Hopefield but not yet issued.

There is also a large intake of water for irrigation, both from the river and from groundwater in the area. Irrigation has not been included in the model due to lack of data but can locally be important.

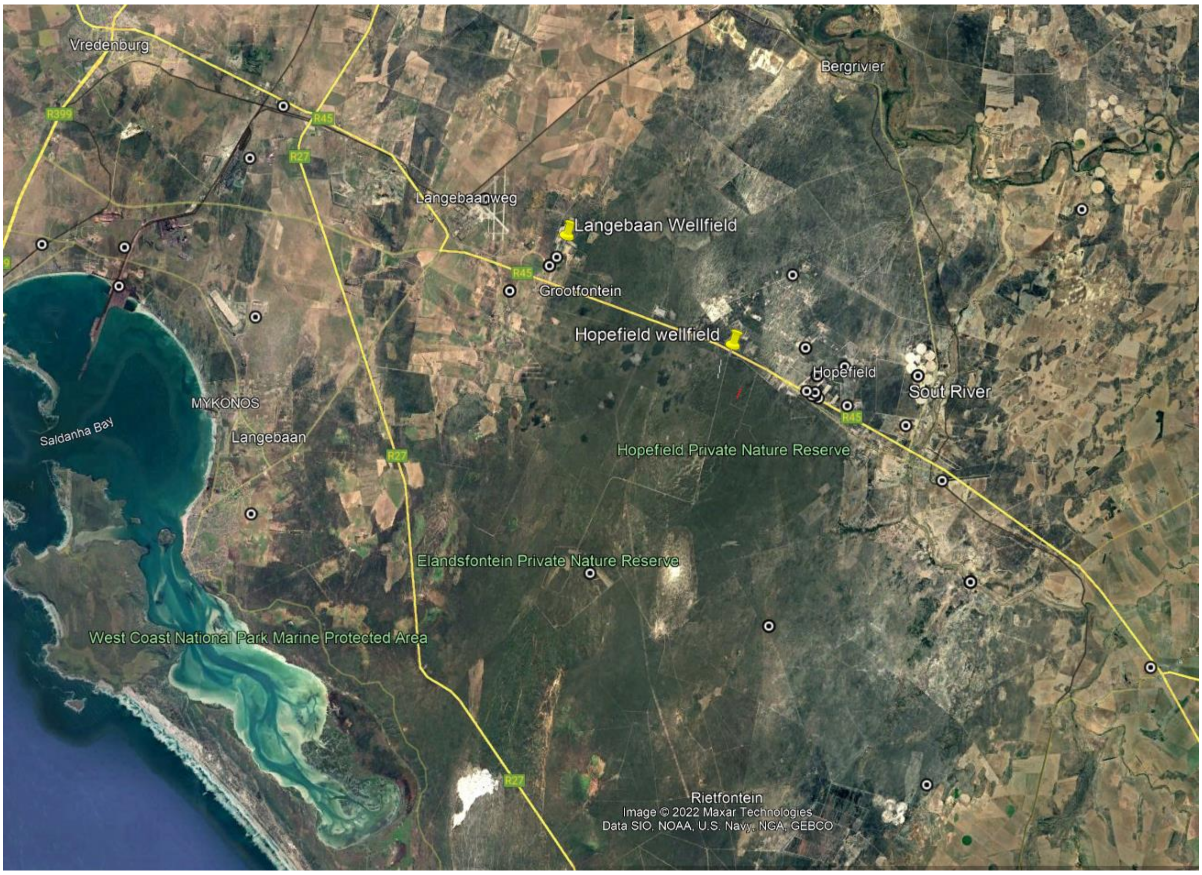

Figure 4 Location of Langebaan Wellfield and Hopefield Wellfield.

3. DATA

3.1 Data sources

Data has been collected from different sources as shown in Table 1, including data collected at local and regional water authorities, the Municipality, Universities, and local consultancies.

Detailed reports and information have been available and appreciated including ref /5//6//8/ and /12/.

Table 1 Overview of collected data and sources

Data		Source
Geological maps		Council of Geoscience (CGS)
Borehole information (800)	Lithologi	Thesis (Nicolette Vermakk), National Groundwater Archieves (DWF)
	Screens	Thesis (Nicolette Vermakk)), National Groundwater Archieves (DWF)
	Hydraulic head measurements	National Groundwater Archieves (DWF), Hydstra (DWF)
	Borehole logs	Reports, Saldanha Municipality
Digital elevation model (DEM)	30 meter grid	GEOSS
Potentiometric head maps		Reports
Climatic data	Precipitation, Potential evaporation	South African Weather Service, DWF
Land use		Western Cape Farm Mapper reports
River discharge measurements	Stations Berg River	Hydstra, DWS Belville, Zutari
River Cross sections	Berg River	DWS, Zutari
Transmissivity	Pump test data	Saldanha Municipality
Groundwater abstraction		WARMS Database (DWF)
Water chemistry		Water Management System (WMS)
Inflow to eustary		Erika Braune, Louise Dobinson, Zutari
GIS-files	Hydrocensus	Saldanha Municipality
	Rivers and dams	GEOSS
	Bulk pipelines	Thesis
Reports		GH reports
		GEOSS
THESIS	Management strategies for the lower Berg Aquifer system, Western Cape	Nicolette Vermakk

3.2 Topography

The topography is based on a DEM with a resolution on 30x30 meters which is aggregated to the model grid resolution of 200 m, as shown on Figure 5 /2/. In the main part of the area the elevation is below 100 meter above sea-level but increases up to almost 1000 meters above sea-level in the highest areas at the north-eastern border of the model area. In the area around Langebaan and Hopefield Wellfields the elevation is 50-100 meters above sea level.

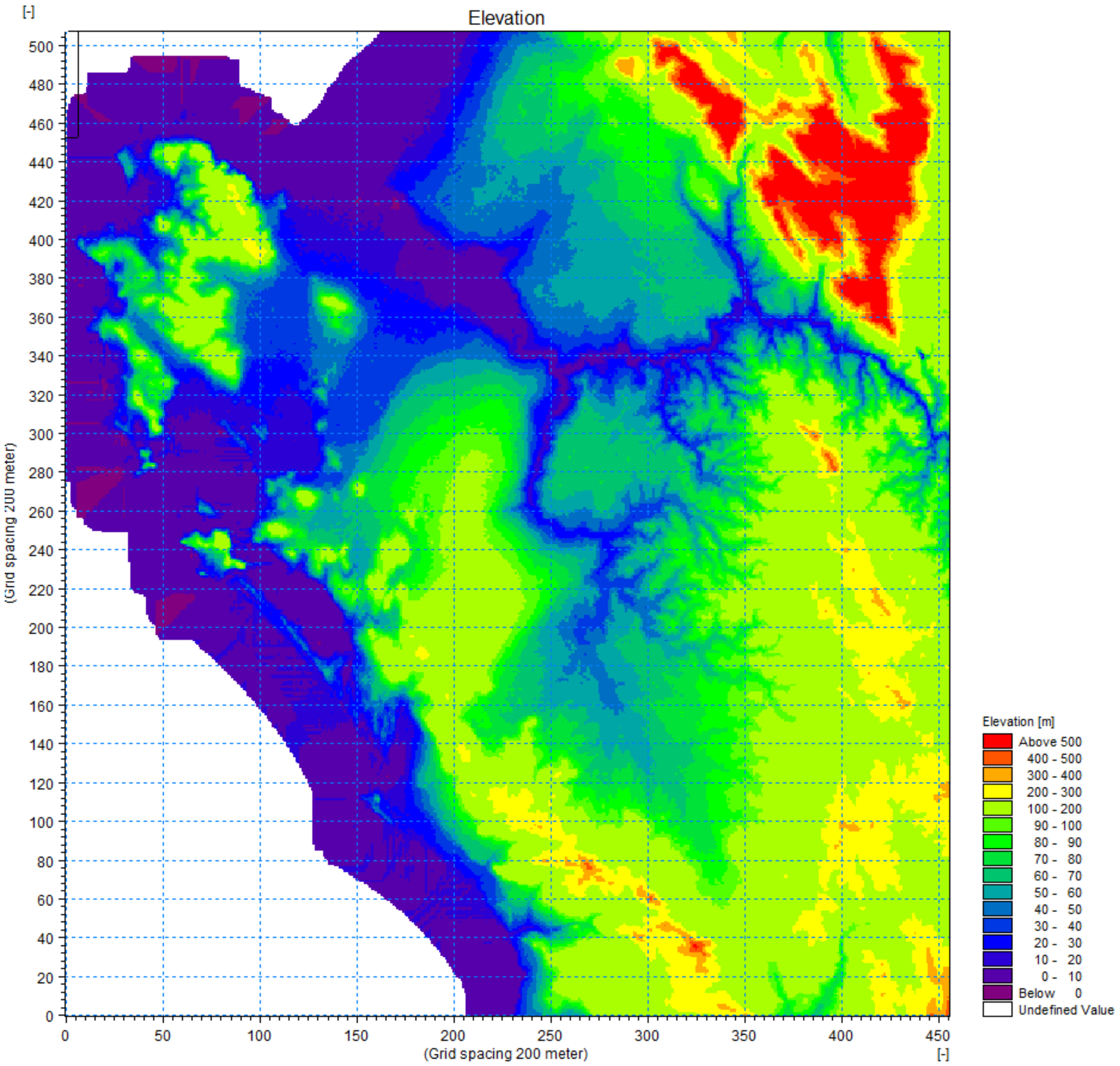

Figure 5 Topography as implemented in the model

3.3 Climate data

Rain and potential evaporation have been included in the model on daily basis. Rain data was available from 5 gauging stations within or near the model area as shown on Figure 6. The active periods from the 5 stations are shown in Table 2 as well as the average annual rainfall

Table 2 Average rain

Station	Period	Average rain 2010-2020 (mm/year)
Atlantis	Since 1979	403
Langebaan	Since 1920	402
Moorreesburg	Since 1969	329
Piketberg SAFD	Since 1920	402
Saldanha Kuspatrollie	Since 2009	292

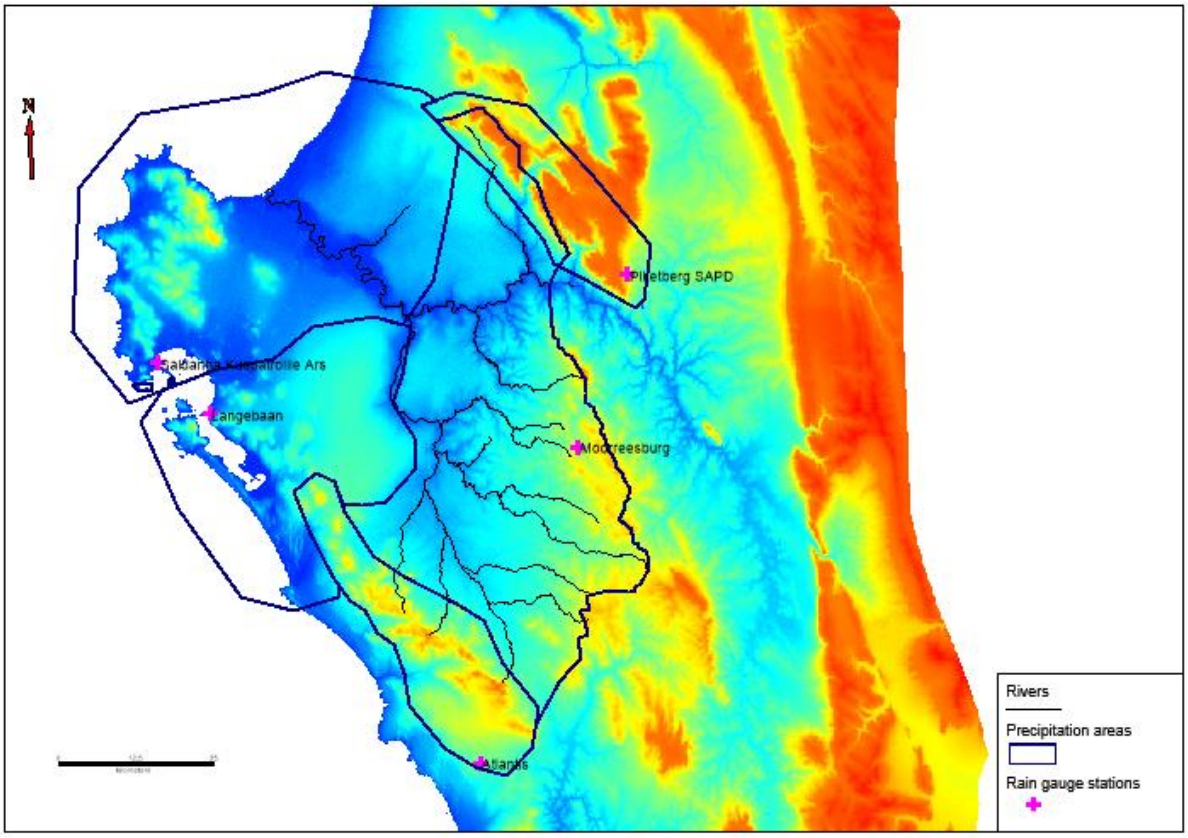

Figure 6 Rain gauge stations and assessed precipitation areas

The precipitation, Figure 7, shows a distinct seasonal pattern with a wet season from May to August and a dry season from September to February. The last decade includes some of the historically lowest annual rainfall with 3-4 years of low rainfall in a row starting in 2015 and ending in 2017/18 (Figure 8), leading to the severe drought in 2018.

The potential evaporation has been translated from monthly evaporation data to daily values for the period 2005-2020 by assuming a gradual increase or decrease in potential evaporation between two monthly values. So, for example if the monthly potential evaporation increased 30 mm from November to December it is assumed that the increase was 1 mm/day and vice versa if the total potential evaporation decreases from one month to the next.

The translated daily values are shown on Figure 9. The average potential evaporation on daily basis is 3.95 mm.

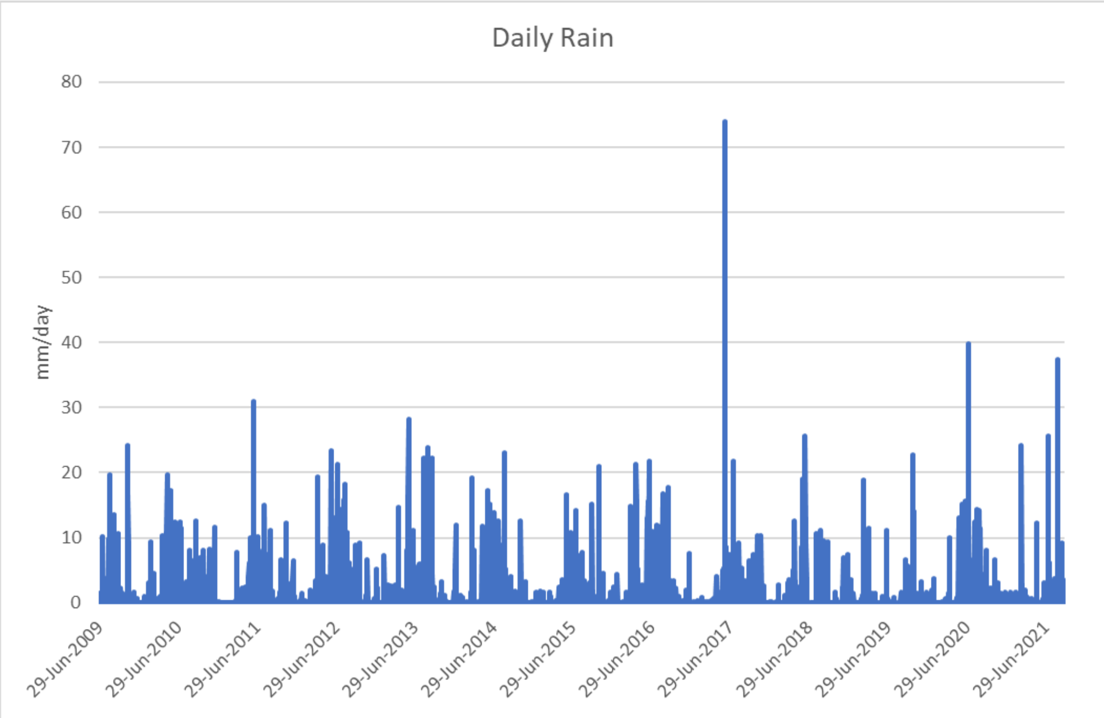

Figure 7 Daily rain at Saldanha

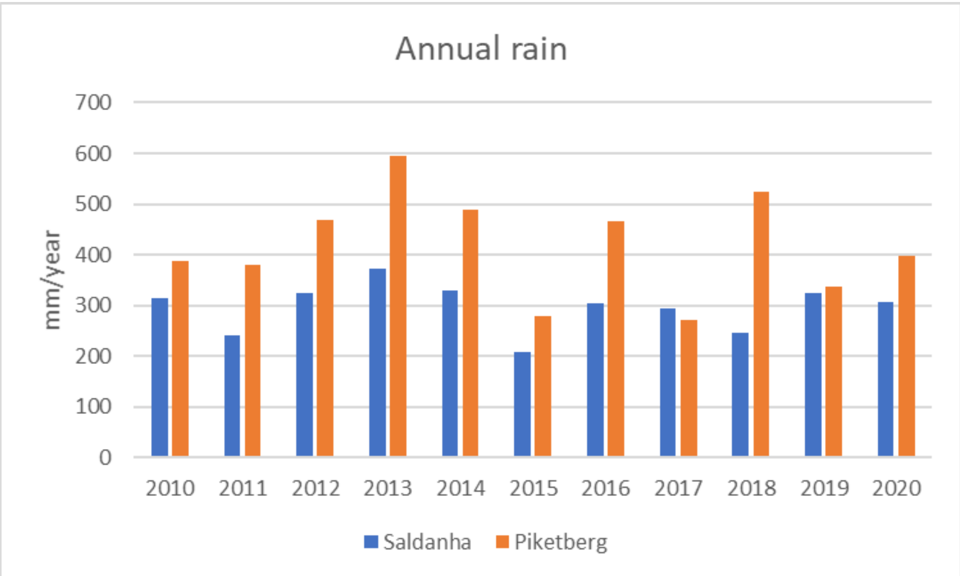

Figure 8 Annual rain at Saldanha and Piketberg

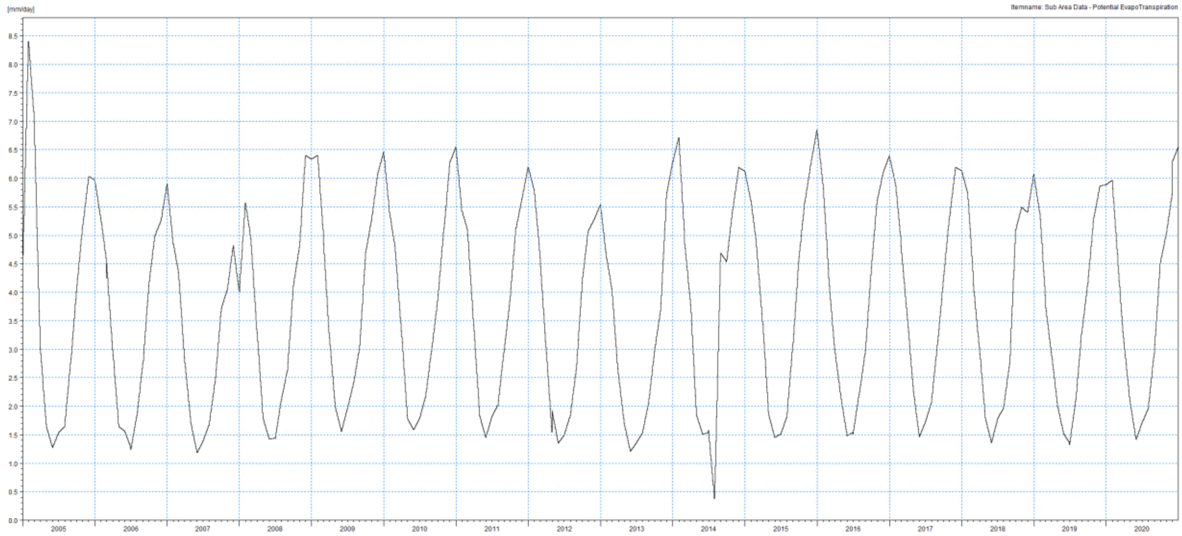

Figure 9 Daily potential evaporation (mm/day).

3.4 Land use and vegetation

Land use and vegetation is shown on Figure 11. The land use within the model area consists mainly of nature and cultivated areas. The vegetation within the cultivated areas consists primarily of pasture and grains. Crops and vegetation are implemented in the model based on the dominant land uses and crops. A total of 5 land uses has been included in the model; nature, urbanized areas, cultivated areas, vineyards, and plantations. Each crop is described by a leaf area index, the root depth and a crop coefficient. An example for grain is shown on Figure 10. Dominant crops have also been included in the sensitivity analysis evaluating its sensitivity regarding groundwater flow.

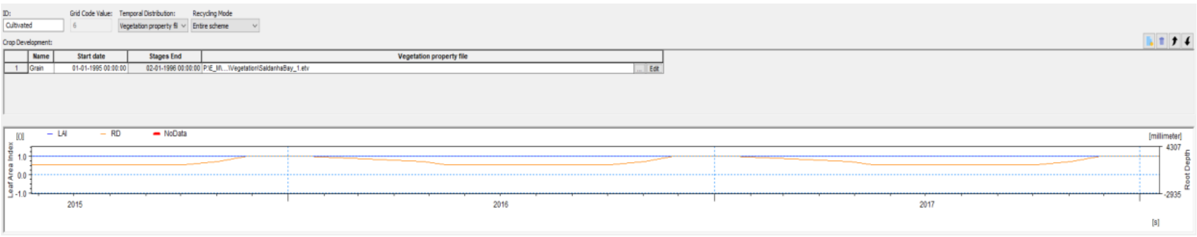

Figure 10 Leaf area index and root depth for grain on cultivated areas

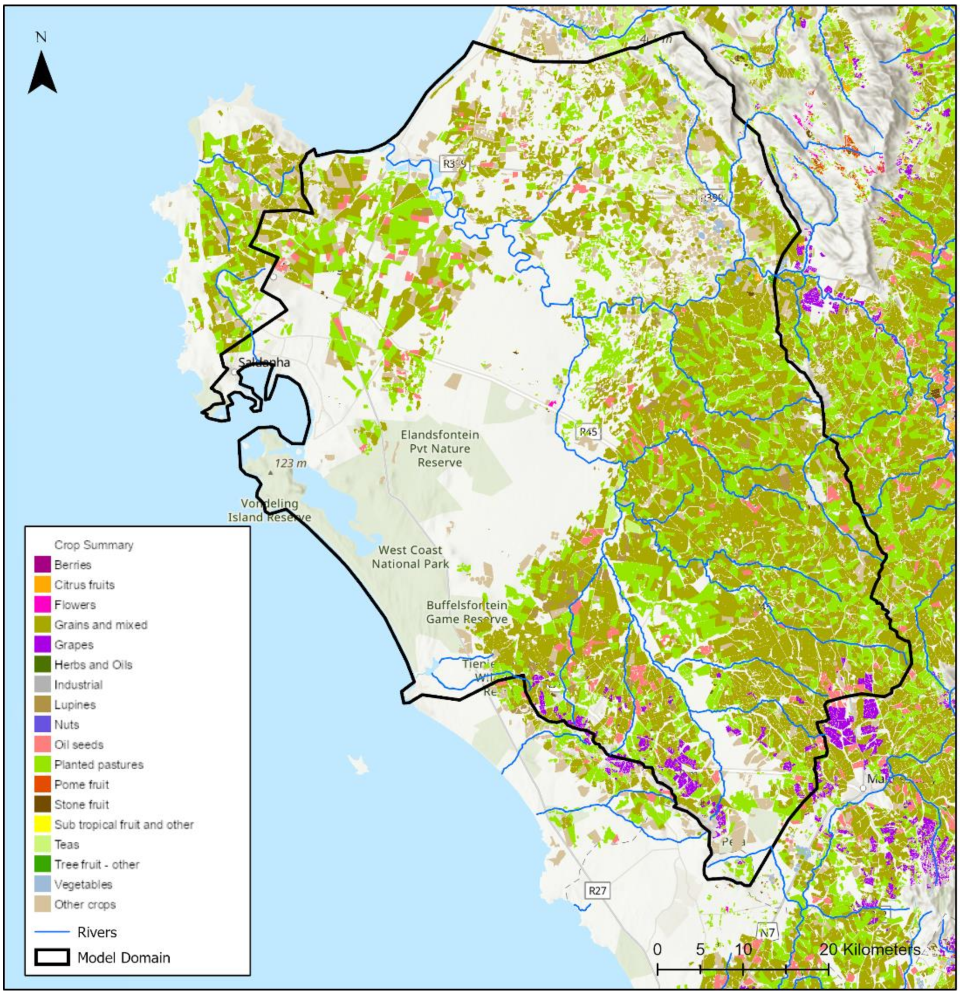

Figure 11 Land use and vegetation.

3.5 Groundwater data

3.5.1 Groundwater abstraction

Groundwater abstraction has been included in the model based on data from the WARM database, supplemented with data on the abstraction permit from the wellfields. For the calibration model only abstraction from Langebaan Wellfield has been included. Based on the Warm Database there is a total license for groundwater abstraction on 8.9 million m^3 per year (exclusive the wellfields) within the model area. The groundwater use is mainly for irrigation and distributed on 72 plants. According to /12/ in 2016 there were a total of 78 registrations in the warm database and a total abstraction on 6.9 million m^3/year in an almost identical study area. According to /12/ one of major challenges is also that there is no information about which aquifer is targeted. Moreover, according to /12/ the number of private boreholes is not fully captured in the Warm database when comparing with the hydro census data.

It has been assumed that most of the private groundwater is abstracting from the upper aquifer. However, it is assumed that some of the private groundwater users abstract from the lower aquifer, where is upper aquifer is thin or missing.

When the abstraction for Langebaan Wellfield id added, the total groundwater abstraction within the model area is 11.9 million m^3/year distributed on 101 wells giving and average of 118.000 m^3/year per well. The location of the implemented wells is shown on Figure 12. This is most likely an overestimation of what is being abstracted, and as described later, it also gave problems during the simulations where the abstraction from the upper aquifer were reduced by 20-25 % because the groundwater level was lowered down to the screens. The actual groundwater abstraction in the model is therefore around 6.9 million m^3/year for irrigation plus the abstraction from the well fields, matching the abstraction in /12/ better. For a specific groundwater user, the license has been evenly distributed on the wells belonging to the groundwater user.

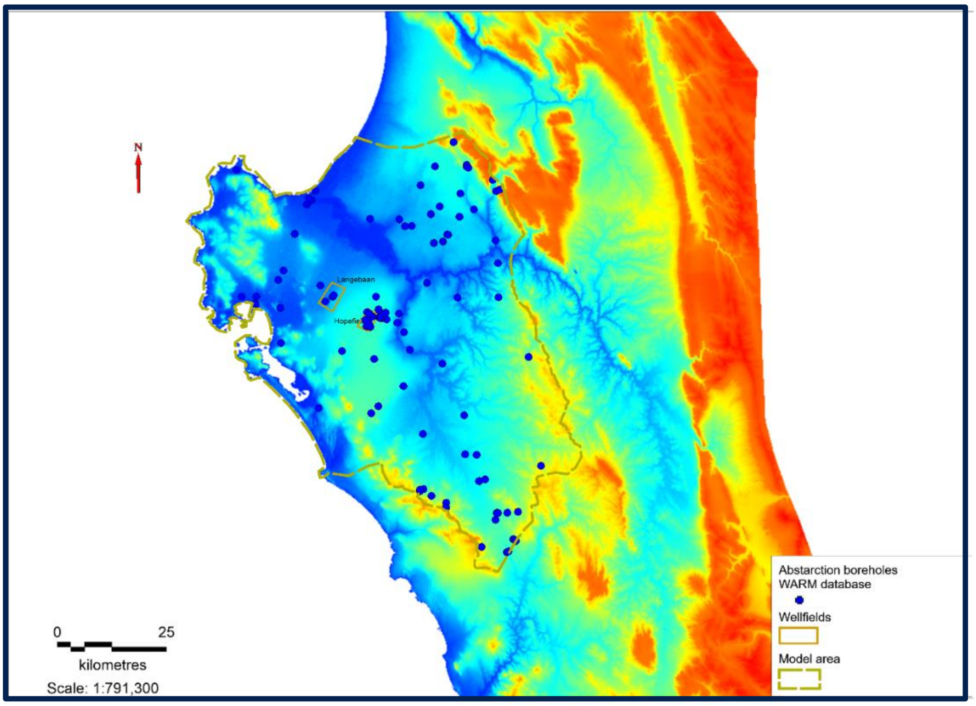

Figure 12 Location of groundwater abstractions as well as Langebaan Wellfield and Hopefield Wellfield

3.5.2 Groundwater head measurements

There is a rather comprehensive network of observation boreholes in the area and both historically and recent time series are available. From Table 3 about 120 boreholes have more than 108 observations.

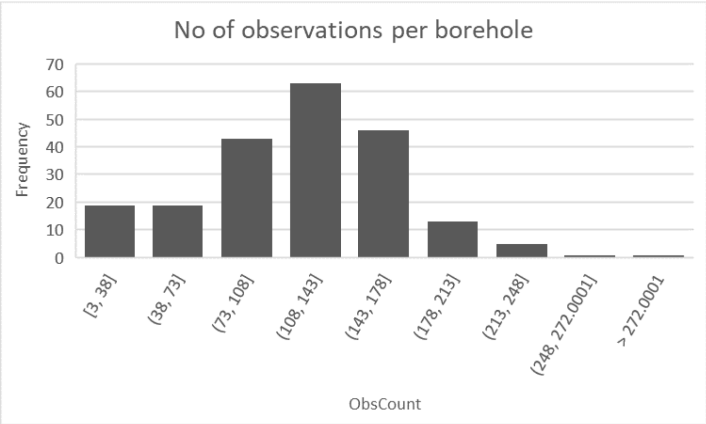

Table 3 No. of observation per borehole

For the model period 2010-2020 a total of 211 observations wells has groundwater head measurements within the period. The locations of the observation boreholes used in the model are shown in Figure 13. It can be seen from the figure that in the central parts of the model area around the wellfields, data are dense while data are sparse at the borders of the model area.

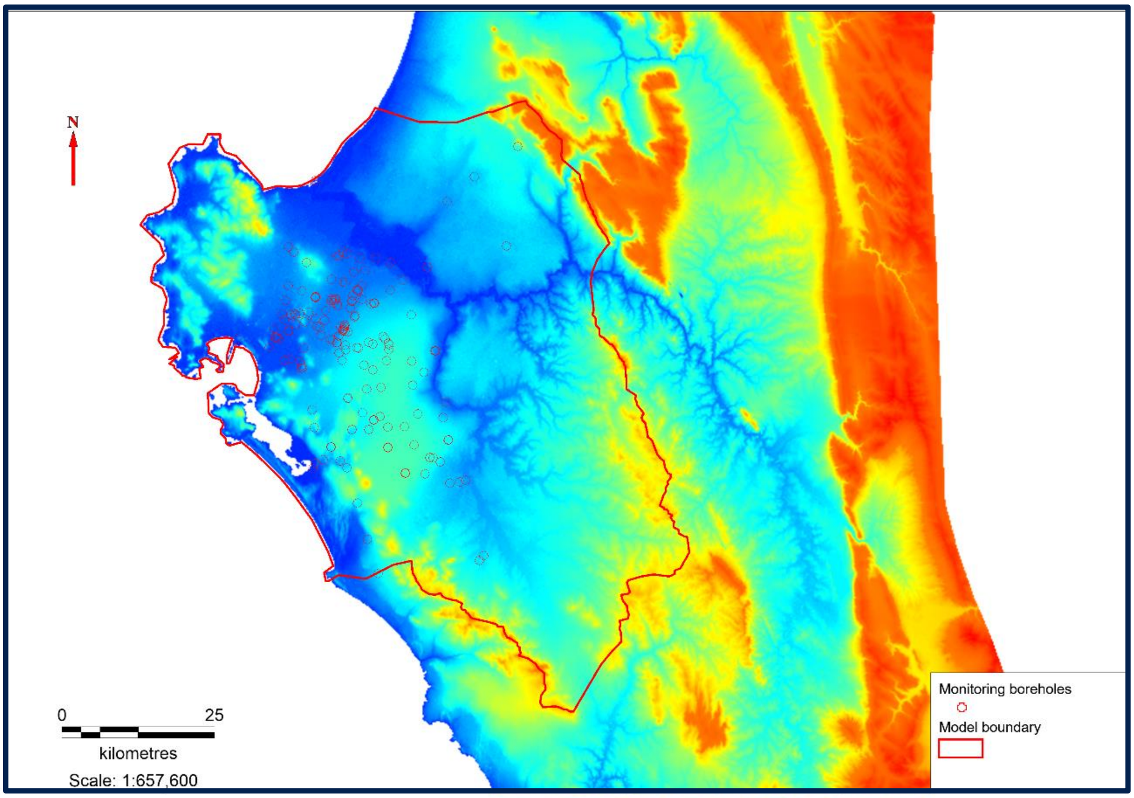

Figure 13 Location of observation boreholes with observations in the period 2010-2020

3.5.3 Test pumps and Aquifer yield

In 1998 step-pump tests were conducted on the wells, G45632, G45633 and G45634 /3/ as shown in Table 4. Based on the total drawdown and yield in the last step the transmissivities were estimated to be approximately 4.81 e-3 m^2/s in G45632 and 1.56 e-3 m^2/s in G45633. In G45634 the transmissivity is not calculated because the static water level is not known. The three boreholes are all located at Langebaan wellfield and screened in the lower aquifer. With a thickness of the lower aquifer between 30 and 40 meters in the area, the hydraulic conductivities can be calculated to 0.00012 m/s and 0.00004 m/s, respectively, which is within the range of medium-fine sand.

Moreover, yield assessments have been conducted at Hopefield Wellfield /12/. The transmissivity has not been extracted from the test, but large drawdowns and low yields indicate a low hydraulic conductivity/transmissivity in the area.

Table 4 Step pump tests

SiteName	ObsSiteName	PumpMethod	DateTimeStart	DateTimeMeas	WaterLevel	PumpRate	Comment
demo	demo	P	9/30/2000 12:00	9/30/2000 12:00	-1.00	-1.00	
G45632		P	1/29/1998 7:00	1/29/1998 7:00	9.16		Static WL
G45632		P	1/29/1998 7:00	1/29/1998 8:00	9.73	10.3	STEP_1
G45632		P	1/29/1998 8:00	1/29/1998 9:00	10.54	20.8	STEP_2
G45632		P	1/29/1998 9:00	1/29/1998 10:00	11.23	26.8	STEP_3
G45632		P	1/29/1998 10:00	1/29/1998 11:00	12.67	36.1	STEP_4
G45632		P	2/1/1998 5:55	2/1/1998 5:55	9.13		Static WL
G45632		P	2/1/1998 5:55	2/1/1998 6:00	12.27	29.4	CONST. YIELD
G45632		P	2/1/1998 5:55	2/1/1998 12:40	9.7		CONST.YIELD
G45633		P	1/29/1998 7:00	1/29/1998 7:00	3.29		
G45633		P	1/29/1998 7:00	1/29/1998 8:00	4.39	10.5	STEP_1
G45633		P	1/29/1998 8:00	1/29/1998 9:00	7.15	20.9	STEP_2
G45633		P	1/29/1998 9:00	1/29/1998 10:00	9.4	26.8	STEP_3
G45633		P	1/29/1998 10:00	1/29/1998 11:00	13.5	35.9	STEP_4
G45633		P	1/31/1998 7:55	1/31/1998 7:55	3.29		
G45634		P	1/31/1998 7:55	1/31/1998 8:00	12.4	28.9	CONST. YIELD
G45634		P	1/29/1998 7:00	1/29/1998 7:00		8.03	
G45634		P	1/29/1998 8:00	1/29/1998 8:00	10	9.19	STEP_1
G45634		P	1/29/1998 9:00	1/29/1998 9:00	20.6	11.32	STEP_2
G45634		P	1/29/1998 10:00	1/29/1998 10:00	26.6	12.7	STEP_3
G45634		P	1/29/1998 11:00	1/29/1998 11:00	35.9	15.24	STEP_4
G45634		P	1/31/1998 8:00	1/31/1998 8:00	28.7	14.13	CONST.YIELD
G45634		P	1/31/1998 8:00	1/31/1998 13:00	28.7	8.6	CONST.YIELD

3.6 River data

The rivers implemented in the model are shown on Figure 14. All the implemented rivers, except for Berg River, are ephemeral, and has its source within the model area.

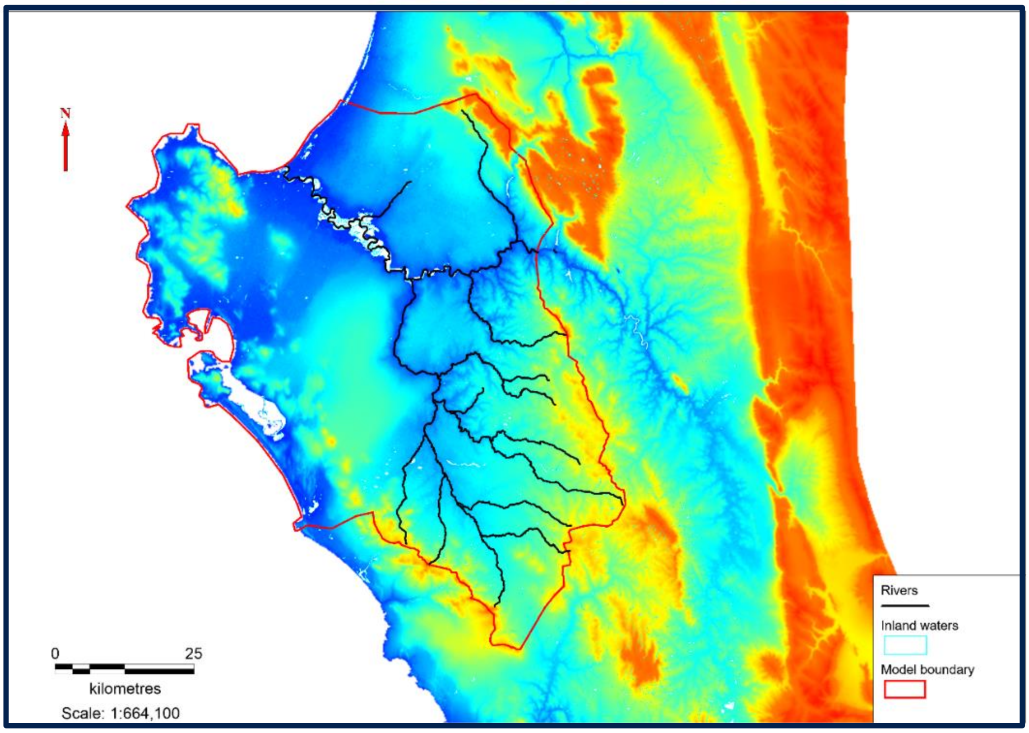

Figure 14 Location of rivers implemented in the model

4. MODEL CONSTRUCTION

4.1 Model period, timestep and grid size

The model was calibrated for the period from 2010 to 2020 using a timestep of 1 day. The period contains both wet and dry years, especially it is worth to mention that the period contains the 3 dry years (2015-2017) responsible for the severe water crisis in 2018 in the area.

The model has been run with 2 different grid sizes 200x200 meters and 400x400 meters, respectively. The 200-meters grid size model is the basic model, but due to very long simulation times, the calibration has been carried out using the 400-meter grid size model. Afterwards it has been ensured that the model accuracy is the same in the 200-meters model as in the 400-meters model, before the 200-meter model was used for the scenario runs.

4.2 Boundary conditions

The model contains two types of boundaries: a fixed head boundary at the Atlantic Ocean and a zero-flux head boundary at topographic divides or along a flowline as the northernmost boundary. The fixed head boundary has been with a head on zero representing the sea. The same outer boundary has been implemented for all layers and are shown in Figure 16. Where Berg River enters the model area, there has been implemented an inflow boundary in MikeHydro River.

There is no straight relationship between the amount of rain and the elevation (lowest rain often expected in lowest areas), therefore a division of the area into zones with equal precipitation based on Thiessen polygons may be a reasonable approach. Nevertheless, there is a fairly big difference in the amount of rain between the Langebaan and Saldanha Kuspatrollie gauging stations located close to each other, which cannot be attributes to physical properties directly, and Thiessen polygons has thus not been used directly. Langebaan gauging station is assessed to represent the higher elevated dune areas, while the Saldanha Kuspatrollie gaugin station is assumed to present the lowest parts of the area. In the delineation of the other areas, the topography has also been used to make the delineations. Each gauging station has been assigned a precipitation zone.

As mentioned earlier, the abstraction wells have been implemented based on information from the WARM database. The challenge has been to locate the screens of the wells at the right depth, and for each well the screen depth has been assessed by an individual judgement based on available aquifers at the specific locations. An example of screening is shown on Figure 15.

Another issue is that, because a great part of the abstraction is for irrigation, a part of the irrigated water will go back into the hydrological system. This has not been addressed in the current model setup as well as the seasonal variation in groundwater abstraction for irrigation.

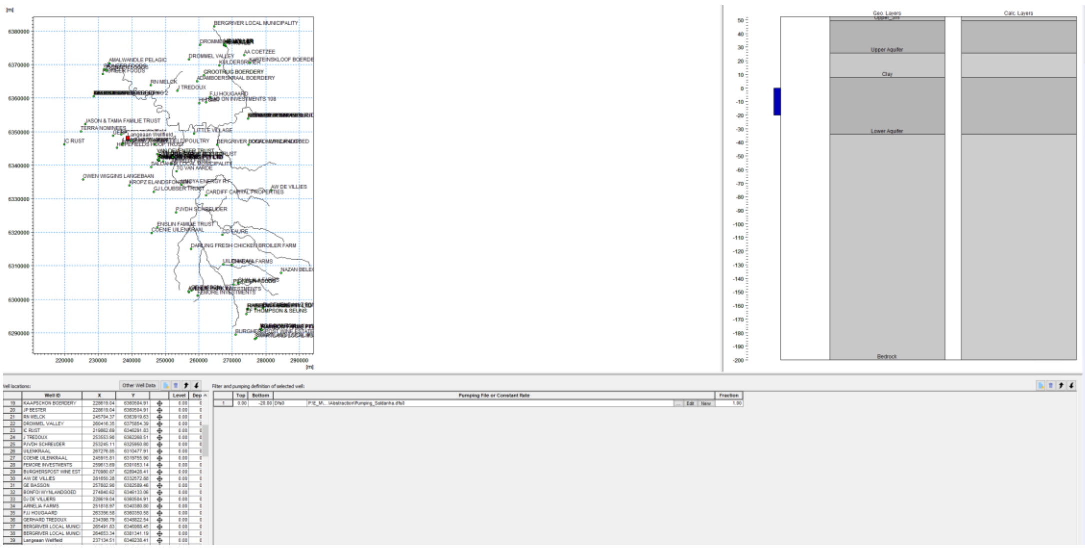

Figure 15 Screening of abstraction boreholes, here an example from Langebaan Wellfield.

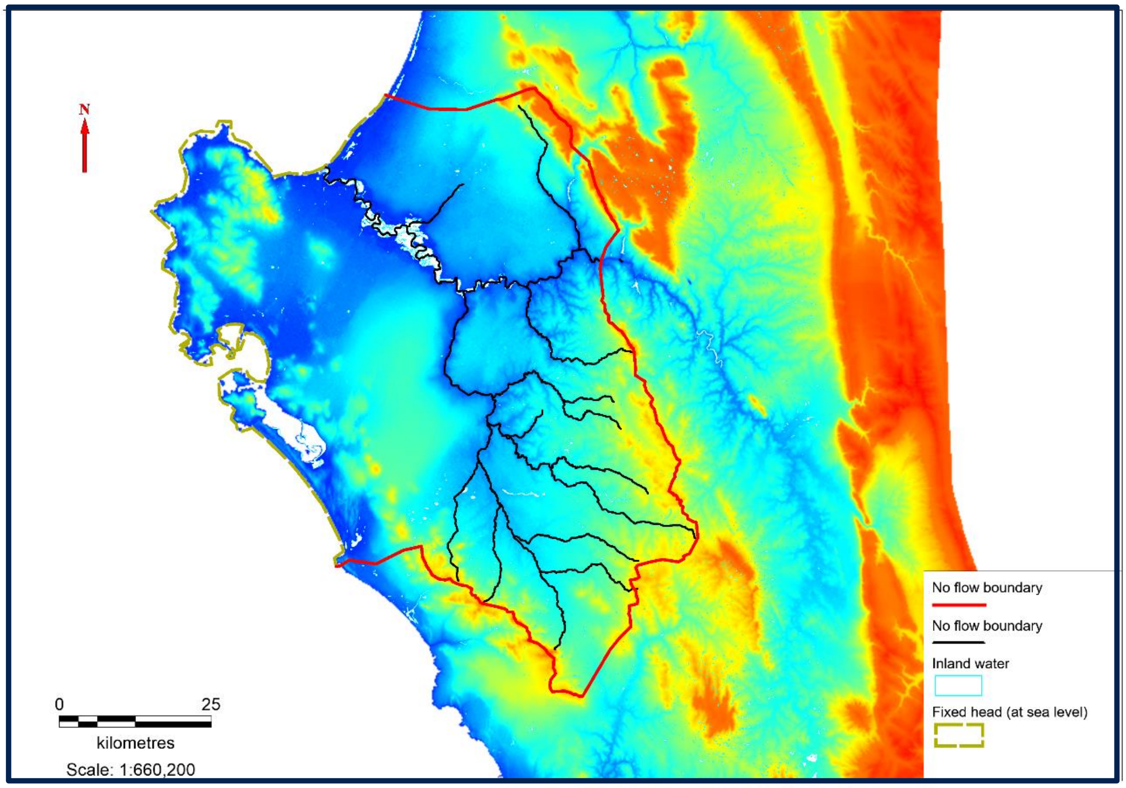

Figure 16 Outer boundary conditions

4.3 Hydro stratigraphical model

The focus has been in defining a hydro stratigraphical model mapping layers with similar hydraulic properties and with less focus on the geological stratigraphy. But, as described below, there is generally a good correspondence between the two model types in the area. For more information about the geological model can be found in /11/.

The hydro stratigraphical model consists of 4 layers:

1. The Upper aquifer
2. A clay unit separating the upper and lower aquifer
3. The Lower aquifer
4. The Bedrock

The upper aquifer contains several formations, including sand members from the Varswater Formation and the Langebaan and Witzsand Formations. The lower aquifer is the Elandsfontyn Formation while the clay layer is the Langeenheid Clay Member in the lowest part of the Varswater Formation. The clay unit also contains the most upper part of the Elandsfontyn Formation where it becomes clayey and peaty.

The upper aquifer is both of aeolian and fluvial origin while the lower aquifer is of fluvial origin.

The bedrock consists primarily of granite and shale from the Malmesbury Formation.

4.4 Hydraulic zones in the model

The layers in the model have been zoned according to the distribution of the geological formations /8/ as shown on Figure 17 except for the clay unit, which has been zoned both with regards to the distribution of the geological formations as well as the thickness of the layer. Where the thickness of the clay layer is less than 0.5 meters (the minimum layer thickness according to the interpolation of the layers) the layer has been giving the same hydraulic properties as the upper aquifer. The zones in the clay unit are shown on Figure 18.

The distribution of the hydraulic properties in the lower aquifer is shown on Figure 19. The aquifer is present in most of the model area, except in elevated areas dominated by hard rock. The distribution of the hydraulic properties in the bedrock is shown on Figure 20. The bedrock is dominated by granite, shale and greywacke.

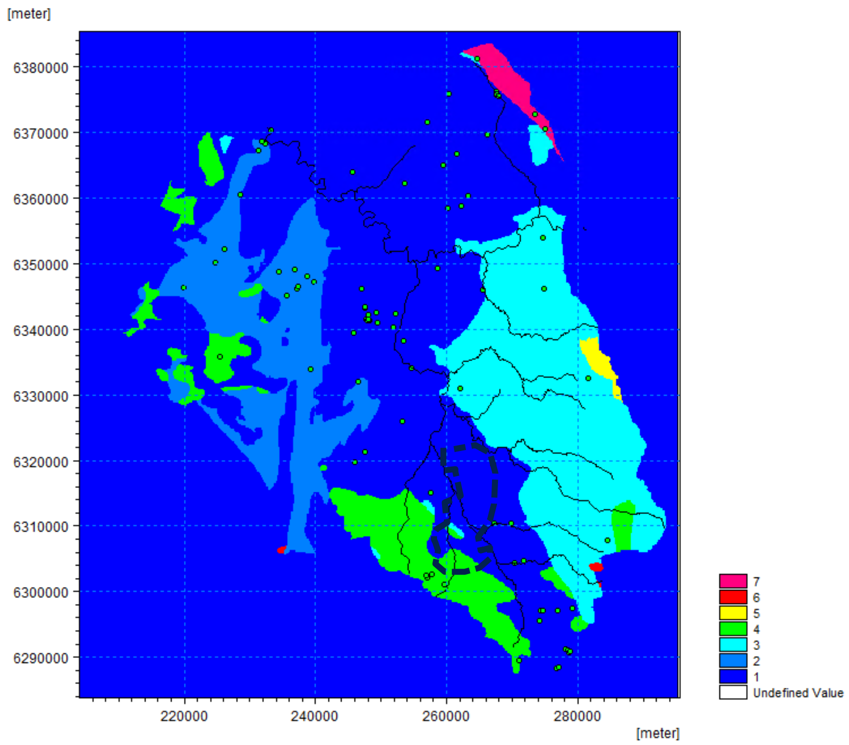

Figure 17 Hydraulic Zones in layer 1 in the model. 1: Upper Aquifer, 2: Upper aquifer-Sandvel limestone: 3: phyllitic shale, Greywacke and sandstone 4: Granite, 5: Schist, 6: Diorite, 7: Sandstone: 22: Dotted polygon – zone with an assumed higher hydraulic conductivity in the upper aquifer

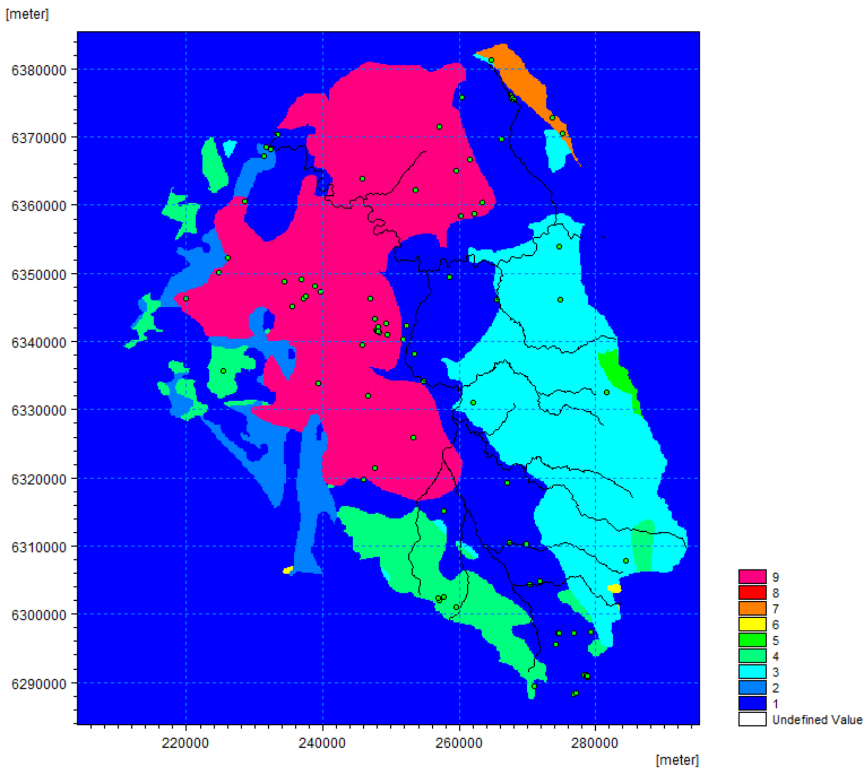

Figure 18 Hydraulic zones in the clay unit (layer 2). 1: Upper Aquifer, 2: Upper aquifer: (Sandvel formation: 3: phyllitic shale, Greywacke and sandstone 4: Granite, 5: Schist, 6: Diorite, 7: Sandstone, 8: Not used, 9: Clay

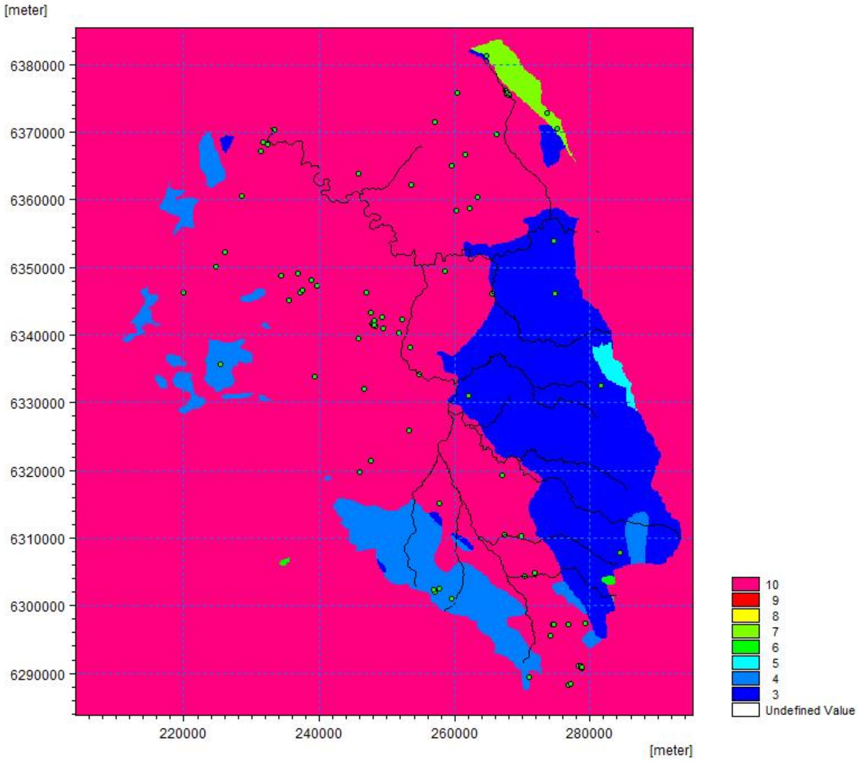

Figure 19 Hydraulic Zones in layer 3 (the lower aquifer). 3: phyllitic shale, Greywacke and sandstone, 4: Granite, 5: Schist, 6: Diorite, 7: Sandstone, 8: not used, 9: not used, 10: Lower aquifer sandy deposits

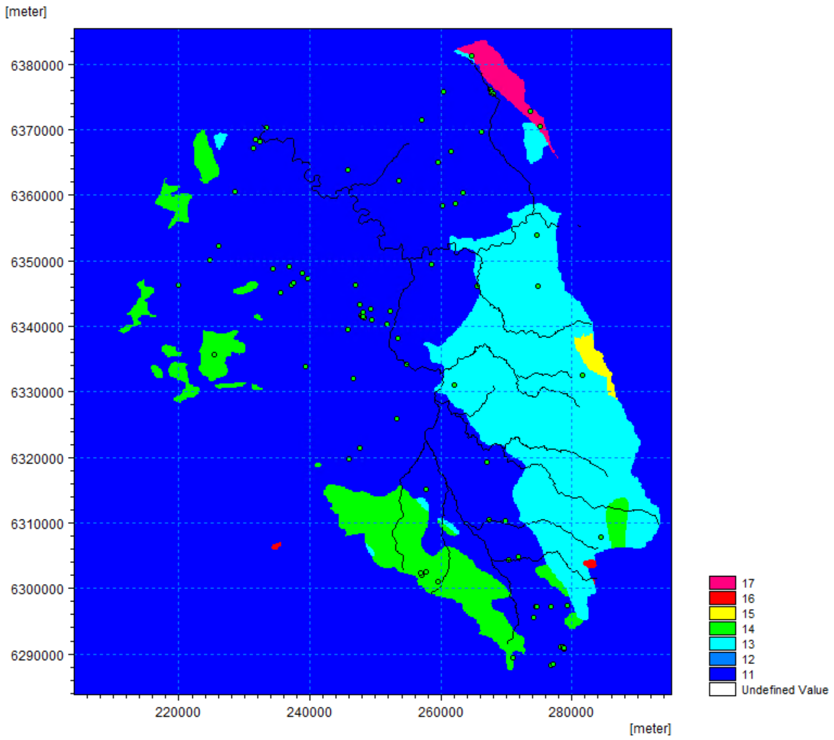

Figure 20 Hydraulic Zones in layer 4 (the bedrock) in the model. 11: Granite/shale 12: not used, 13: phyllitic shale, Greywacke and sandstone, 14: Granite, 15: Schist, 16: Diorite, 17: Sandstone

4.5 Unsaturated zone

The 2-layer model has been used to describe the unsaturated zone in the model. The hydraulic parameters in the unsaturated zone have been distributed according to the distribution of the geological formations as shown on Figure 21.

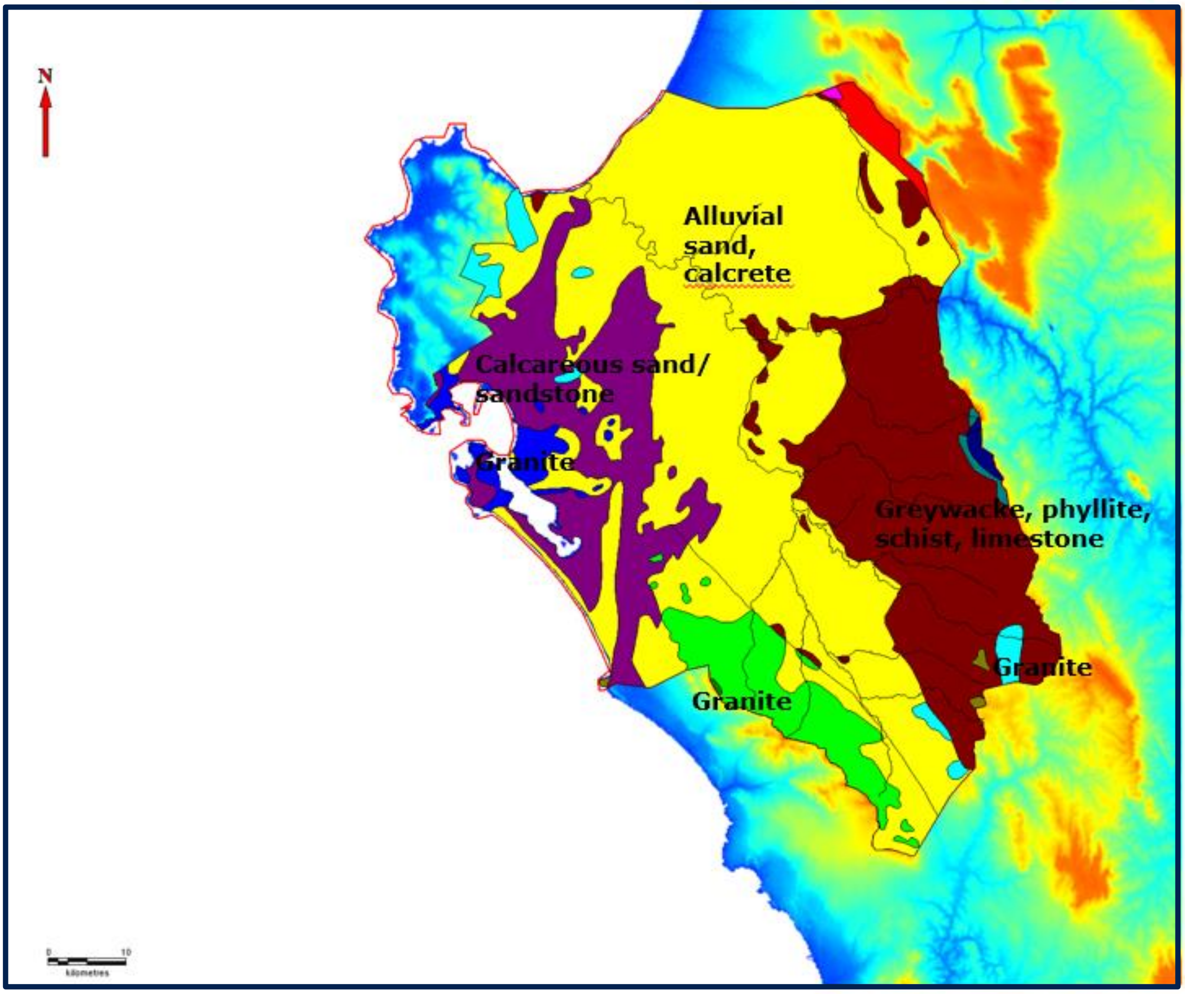

Figure 21 The hydraulic zones for the description of the unsaturated zone.

4.6 Implementation of groundwater head measurements

Groundwater head measurements from 211 observation boreholes have been included in the model. The biggest challenge has been to identify the correct screen depths, as information on this was only available for 49 observation boreholes. Therefore, for the remaining observation boreholes the screen depths have been estimated based on the hydro stratigraphical model applying the following rules:

1. In areas where the lower aquifer is present it is assumed that the borehole is screened in the lower aquifer
2. In areas where the lower is not present it is assumed that it is screened in the upper aquifer
3. In areas where neither the upper aquifer nor lower aquifer is present it is screened in the bedrock

This will of course introduce a higher uncertainty in the model performance if the observations are misplaced in the model and model simulations thus are compared to head elevation in a different aquifer.

4.7 Implementation of rivers

Artificial cross sections have been implemented for all other rivers, except for the lower part of Berg River, based on google earth measurements of river widths and defined for every 2000 meter. The locations of all the cross sections are shown in Figure 22. Generally, the artificial cross sections have a width of 5-10 meters and a depth of a few meters.

For Berg River, cross sections have been available for the lower part as shown in Figure 23. An example is shown on Figure 24. The cross sections are much wider compared to the ephemeral rivers. At the lower part of Berg River at the estuary the river flows within a broader area of inland water, where previous meandering of the river has created a broader wetland area.

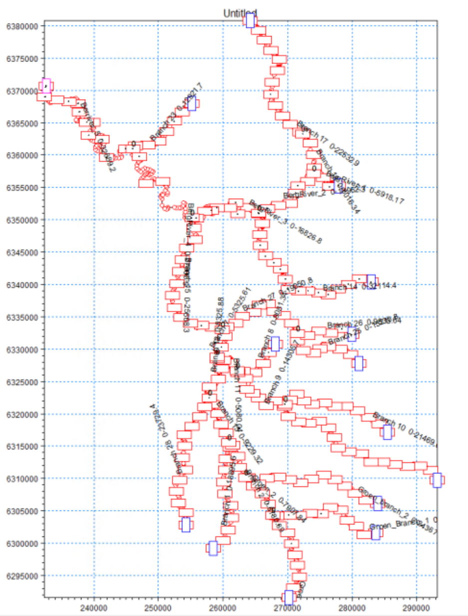

Figure 22 River cross sections included in the model

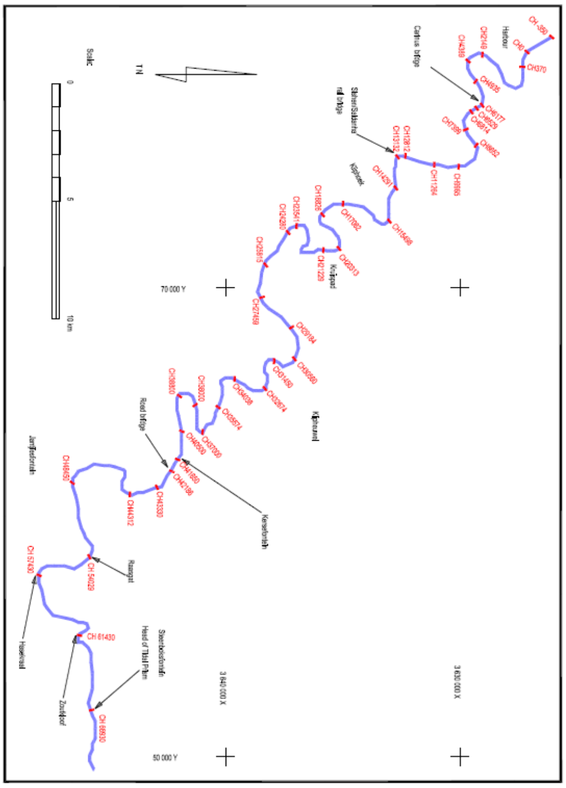

Figure 23 Location of measured river cross sections in the lower part of Berg River /9/

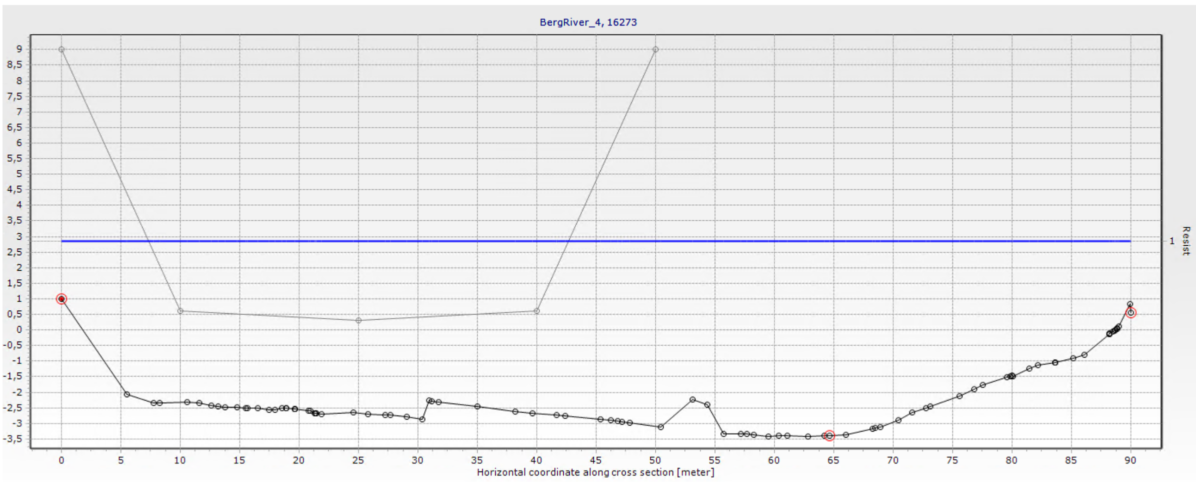

Figure 24 The lowest cross section is an example of an implemented cross section at the lower part of Berg River. The highest cross section is an artificial cross section where Berg River enter the model area.

The rivers have been implemented in Mike Hydro River and dynamically coupled to MIKE SHE. Mike Hydro River can simulate the flow in the rivers based on different wave equations. For this project simple routing has been selected because it is a stable and fast method, the disadvantage is that it can't simulate backwater from the sea related to the tidal water

00

Figure 25 Location of River Discharge Stations at Berg River

In Berg River there are several discharge stations as shown on Figure 25 and in Table 5. The measured river discharge at station G1H031 has been used as input (Boundary) to Berg River because it is located close to where Berg River enters the model. The measured discharge at the station is shown on Figure 26.

Table 5 River discharge stations

Order	Station ID	Name	Catchment	Lat	Long	WWW			Long
1	G1H075	Berg River at Misverstand	3972	-33.0238	18.78855	https://www.dws.gov.za/Hydrology			18.78855
2	G1H031	Berg River at Die Brug	3984	-32.9969	18.77889	https://www.dws.gov.za/Hydrology			18.77889
3	Calculated inflows	Based on observed flows G1H031 and takes into account irrigation abstractions and catchment inflows							
4	G1H023	Berg River at Jaantjiesfontein	6925	-32.9461	18.33694	https://www.dws.gov.za/Hydrology			18.33694
5	G1H024	Berg River at Kliphoek	7870	-32.8142	18.19472	https://www.dws.gov.za/Hydrology			18.19472

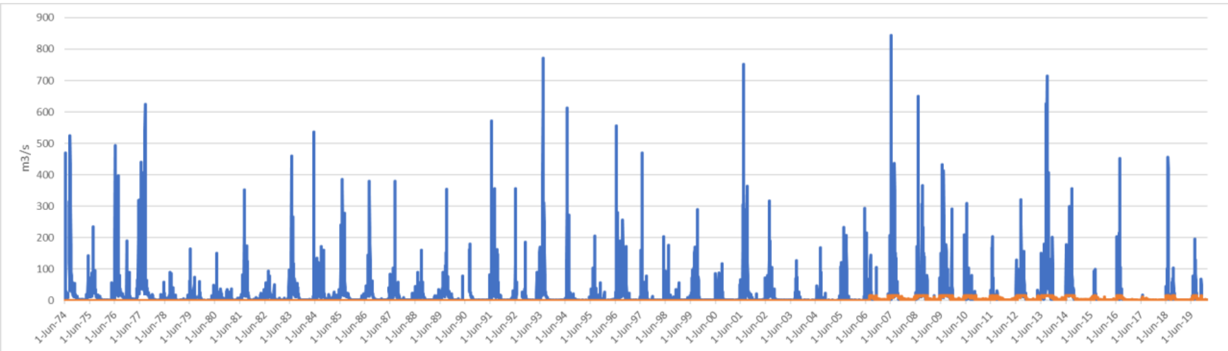

Figure 26 Measured River discharge at station G1H031

The exchange between groundwater and the rivers is described by a leakage coefficient. This coefficient has been included in the calibration of the model.

5. CALIBRATION AND VALIDATION

5.1 Initial hydraulic parameters

Prior to the calibration the hydraulic zones were given initial values. Each hydraulic zone was initially given a hydraulic parameter characteristic for the lithology which is shown in Table 7 and Table 6. Those who came out as sensitive were adjusted during the calibration, not sensitive parameters were kept on the initially value.

For the bedrock, the hydraulic conductivity was initially set to a higher value than the vertical hydraulic conductivity in the saturated zone, to represent the weathered zone. Moreover, there is distinguished between more shallow (assumed) fractured bedrock and

Table 6 Initial hydraulic conductivities in the unsaturated zone

Lithology	k (m/s)
Alluvium	1.00E-05
Greywacke	2.00E-06
Granite	5.00E-07
Schist	5.00E-07
Diorit	5.00E-07
Sandstone	5.00E-07
Sandvel	1.00E-05

Table 7 Initial hydraulic parameters for the saturated zone

	Kx (m/s)	Kz (M/s)	Specific yield	Specific storage
Alluvial, Upper aquifer	1.00E-04	1.00E-05	0.2	1.00E-05
Sandvel deposits (Witssand Formation)	1.00E-04	1.00E-05	0.2	1.00E-05
Greywacke	2.00E-06	2.00E-06	0.08	1.00E-05
Granite	5.00E-07	5.00E-08	0.05	1.00E-05
Schist	3.00E-07	3.00E-08	0.05	1.00E-05
Diorit	3.00E-08	3.00E-08	0.05	1.00E-05
Sandstone	2.00E-06	2.00E-07	0.277	1.00E-05
Clay	1.00E-07	1.00E-08	0.1	1.00E-05
LowerAquifer	1.00E-04	1.00E-05	0.2	1.00E-05
Granite_deep	1.00E-08	1.00E-08	0.05	1.00E-05
Bedrock_BSchist	3.00E-07	3.00E-08	0.05	1.00E-05
Bedrock_Diorit	3.00E-08	3.00E-08	0.05	1.00E-05
Sandstone_deep	2.00E-06	2.00E-07	0.05	1.00E-05

5.2 Performance goals

The performance goal is that the model validation complies to a conservative model for simulation of groundwater flow according to the Danish model guide /4/. The performance criteria are shown in Table 8 and relates to how accurate the model simulate the measured potential heads. The highest performance is related to a detail model required when the model must simulate the groundwater flow very accurate. This is of course always wanted but can be difficult to achieve in regional models with a high degree of geological heterogeneity. Therefore, the goal from the start has been to reach a conservative model.

One key parameter in the definitions is ΔhMax describing the max difference in observed heads within the area, meaning that the higher ΔhMax is, the more difficult it is to match all observed heads within the model area.

A second important parameter is ME (mean error) describing the average difference between observed and simulated heads for specific monitoring boreholes. A mean error on for example 2 meters mean that the model in average simulate the groundwater head 2 meters too low (or minus 2 if simulated head is 2 meters too high).

A third important parameters ae RMS (Root mean square) which compared to ME, also have the dynamic fit included to some extent in the equation. The formula is shown in the box below.

Statistics - Root Mean Square. Root Mean Square, RMS is defined as the square root ofmean square where mean square is the arithmetic mean of the squares of numbers. MS is also termed as the quadratic mean. Formula. ${ x_{rms} = \sqrt{ \frac{1}{n} ({x_1}^2 + {x_2}^2 + ... ${x_i}$ = items under observation.

In the higher areas, the max observed groundwater head measurements are above 100 meters giving a ΔhMax of 105 meters. Using this value results in the performance criteria shown in Table 9. No performance goal was set for simulation of the river flows because this was regarded as too uncertain.

Table 8 Performance criteriums according to the Danish model guide/4/

		Screening model	Conservative model	Detail model
Criterium 1	ME/ΔHmax	0.05	0.025	0.01
Criterium 4	RMS/ΔHmax	0.1	0.05	0.025

Another often used criterium is criterium 4, where the output statistic is related to the standard deviation on the observations as well as assessed uncertainties for example related to the geological heterogeneity.

Table 9 Performance values to comply with a screening model, conservative model and detail model, respectively, for the Saldanha Bay hydrological model

		Screening model	Conservative model	Detail model
Criterium 1	ME	5.5	2.625	1.05
Criterium 4	RMS	10.5	5.25	2.625

5.3 Sensitivity analysis and selection of calibration parameters

60 model parameters were included in the sensitivity analysis, including parameters from the saturated and unsaturated zone, vegetation parameters, overland flow (manning number) and

river parameters. The results from the sensitivity analysis are divided in sensitivity for groundwater flow and river discharge, respectively.

Figure 27 shows the sensitivity of the most sensitive model parameters with respect to groundwater, and it can be seen that the model is most sensitive to the horizontal hydraulic conductivity in the upper and lower aquifer, as well as vertical hydraulic conductivity in the separating clay unit.

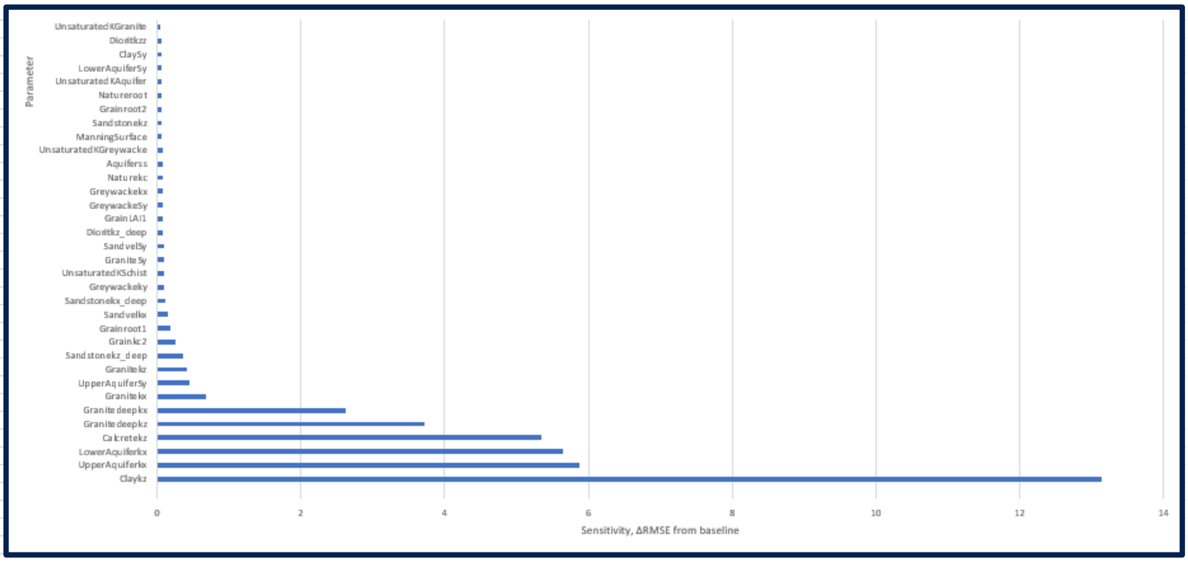

Figure 27 Sensitivity with respect to groundwater, detailed view

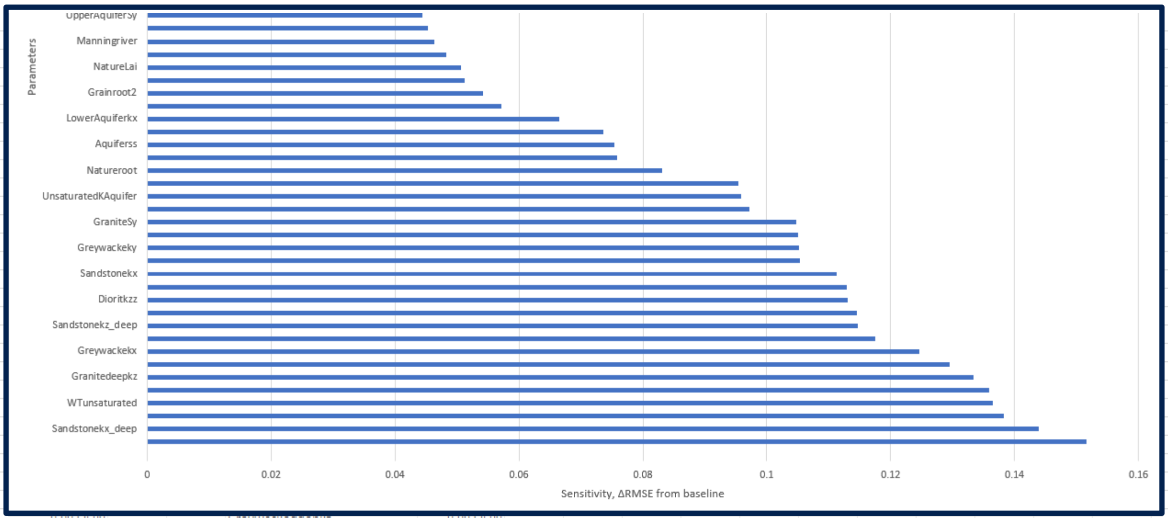

Figure 28 Most sensitive parameters with respect to river flow, detailed view

Parameter sensitivities related to river flow are more diffuse as shown on Figure 28, with many parameters having comparable sensitivities. The most sensitive parameters are the leakage coefficient which mainly describes the character of the river bottom sediments. The selection criteria for calibration were that parameter sensitivity should be more than 5 % of the highest sensitivity. Based on this criterium 30 parameters were selected for calibration shown on Table 10, representing all the domains in the model – the saturated zone, the unsaturated zone, overland flow, the root zone (evapotranspiration) as well as the river.

Table 10 Parameters selected for calibration

Parameter	Description
ManningSurface	Manning number for overland low
WTunsaturated	Water content at saturation
UnsaturatedKAquifer	Hydraulic conductivity unsaturated zone
UnsaturatedKSandstone	Hydraulic conductivity unsaturated zone
UnsaturatedKSandvel	Hydraulic conductivity unsaturated zone
UpperAquiferkx	Hydraulic conductivity saturated zone
UpperAquiferSy	Specific yield
Aquiferss	Specific storage
Sandvelkx	Hydraulic conductivity saturated zone
Greywackekx	Hydraulic conductivity saturated zone
Greywackekz	Verticale conductivity saturated zone
GreywackeSy	Specific yield
Bedrockss	Specific storage
Granitekx	Hydraulic conductivity saturated zone
Granitekz	Verticale conductivity saturated zone
Sandstonekx	Hydraulic conductivity saturated zone
Sandstonekz	Verticale conductivity saturated zone
Calcretekz	Verticale conductivity saturated zone
Claykz	Verticale conductivity saturated zone
LowerAquiferkx	Hydraulic conductivity saturated zone
Granitedeepkx	Hydraulic conductivity saturated zone
Granitedeepkz	Verticale conductivity saturated zone
Greywackeddepkx	Hydraulic conductivity saturated zone
Greywackeddepkz	Verticale conductivity saturated zone
Grainroot1	Vegetation parameter
Grainroot2	Vegetation parameter
Grainkc2	Vegetation parameter
Natureroot	Vegetation parameter
Tributiaries	Leakage coefficient ehmerale rivers
BergRiver	Leakage coefficient Berg River

5.4 Calibration and validation of the model

The model calibration and validation were carried out as a split-sample test. Data for the period 2015-2019, including the 3 dry years 2015,2016 and 2017, was used for calibration. The validation period is the more wet period 2011-2014. A total of 173 groundwater targets and one river target was used in the calibration and validation of the model.

The automatic calibration in MIKE SHE "AUTOCAL", was used to calibrate the model, see /1/ for a detailed description of AUTOCAL. The automatic calibration converged after 121 model runs and the results are shown in Table 12. By comparing the model results with Table 9, the model complies to a conservative model, meaning that the model simulates the general groundwater flow satisfactorily at aquifer level. At local scale, e.g., for boreholes, deviations between observed and simulated groundwater levels will occur, and the model is assessed to simulate differences more certain than actual groundwater levels.

The calibrated hydraulic parameters for the saturated zone are shown in Table 11. Compared to the initial parameters the calibrated parameters are lower for the unconsolidated sediments. For the Sandvel deposits and the lower aquifer, the calibrated value indicates that the aquifers are dominated by fine sand. The calibrated parameter for the upper aquifer also indicates that the aquifer is dominated by fine sand, but also that the aquifer includes some more clayey parts, which confer with the SKYTEM data. This is also in accordance with the survey from Hopefield Wellfield /7/. Such interbedding clay layers calls for a more complex geological model with more layers, which would be beneficial to include in the future development of a more local and detailed model.

For the clay layer separating the upper and lower aquifer, the calibrated value is a little higher than the initial value but is within excepted range for clay. For the bedrock parameters the calibrated values are in general not far from the initial value.

Table 11 Calibrated hydraulic parameters in the saturated zone

	Kx (m/s)	Kz (M/s)	Specific yield	Specific storage
Alluvial, Upper aquifer	9.82E-06	5.06E-07	0.109	0.000397
Sandvel deposits (Witssand Formation)	4.94E-05	4.94E-06	0.2	0.000397
Greywacke	6.42E-07	7.68E-07	0.103	2.47E-05
Granite	3.46E-07	6.42E-08	0.05	2.47E-05
Schist	3.00E-07	3.00E-08	0.05	2.47E-05
Diorit	3.00E-08	3.00E-08	0.05	2.47E-05
Sandstone	8.65E-06	5.04E-08	0.277	2.47E-05
Clay	2.90E-07	2.90E-08	0.1	0.0001
LowerAquifer	6.50E-05	6.50E-06	0.2	0.000397
Granite_deep	2.32E-07	1.32E-08	0.05	3.71E-05
Bedrock_BSchist	3.00E-07	3.00E-08	0.05	3.71E-05
Bedrock_Diorit	3.00E-08	3.00E-08	0.05	3.71E-05
Sandstone_deep	2.00E-06	2.00E-07	0.277	3.71E-05

The spatial distribution of the mean error is provided in Figure 29 showing a generally high variation. In the lower parts of the area around Langebaan and Hopefield Wellfields as well as in the north-eastern part of the model, mean error is lowest meaning that the model has the best performance in this area. The largest errors are found in the elevated area south of Hopefield Wellfield (the delineated area in Figure 29). The errors are both too high and too low simulated potential heads and therefore, it is assessed that the geological heterogeneity is very high in that area supported by the presence of well-known faults systems in this area /5/.

For the wellfield management system 15 monitoring boreholes listed in Table 13 has been selected as control and monitoring boreholes. The transient model simulations for several of the selected boreholes are shown in Figure 30. How close the simulated heads are on the observed heads varies. There is a general good agreement around the two wellfields, also with respect to the dynamics even though there are some variations from year to year that the model cannot simulate. The annual variation is not large for either the observed or modelled groundwater heads within the simulation period.

Table 12 Calibration and validation results

	Calibration period	Validation period
Mean Error (m)	-0.9	-0.5
RMS	5.36	5.18

Table 13 Boreholes defined at control points

BH NAME	LATITUDE	LONGITUDE	AQUIFER	DEPTH (mbgl)
G46092	-32.94473	18.08762	Upper	28
G46025	-33.01272	18.23847	Unkown	65
G33327	-32.96348	18.12761	Lower	83
G33326	-32.93397	18.27127	Upper	80
G46065	-32.91997	18.29422	Lower	34
BG00054	-32.96146	18.15705	Lower	45
BG00062	-33.04536	18.11176	Bedrock	27
G46031	-33.02411	18.17902	Upper	88
G46030	-33.03527	18.18360	Bedrock	119
G33313	-33.10663	18.12897	Upper	57
BH3	-33.18171	18.14594	Lower	60
BH1A	-33.18602	18.13195	Upper	44
G33501	-33.07463	18.30582	Upper	44
G33498	-33.07605	18.2511	Upper	73
G33246	-32.901	18.33653	Upper	25

The largest errors are within the area south of Hopefield and in a borehole (G48065) close to Berg River. The model simulates the potential head in a nearby borehole (G33326) well, but the model simulates a too quick fall in the groundwater level towards Berg River. This discrepancy could relate to the interaction between Berg River and the aquifer, with the aquifer receiving water from Berg River but this needs to be analysed in greater detail.

Another issue that effects the model simulations is the uncertainty related to the groundwater abstraction. Most of the private groundwater use has been targeted to the upper aquifer but this also have the consequence that some screens run dry during the simulations reducing the actual abstraction in the model with 20-25 %. This is probably also caused by the fact that the private abstraction in the model is over-estimated. To increase the model performance actual abstractions rates from individual boreholes should be included and based on information from hydrocensus which according to /12/ should be more accurate. Inclusion of an irrigation module in the model system could probably also improve the performance on local scale.

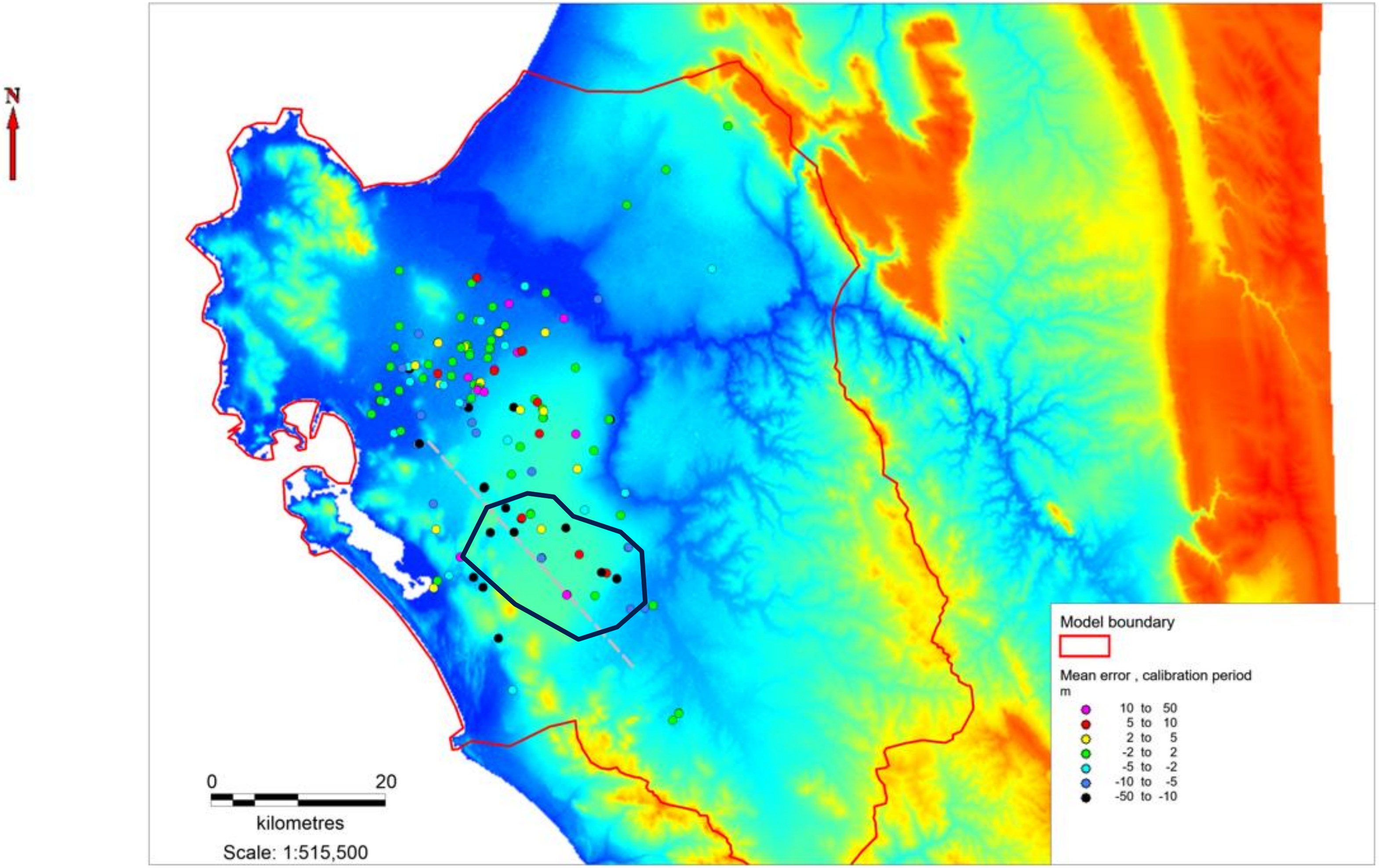

Figure 29 Distribution of mean error. The biggest error is within the delineated area probably disturbed by a fault as indicated by the punctured line

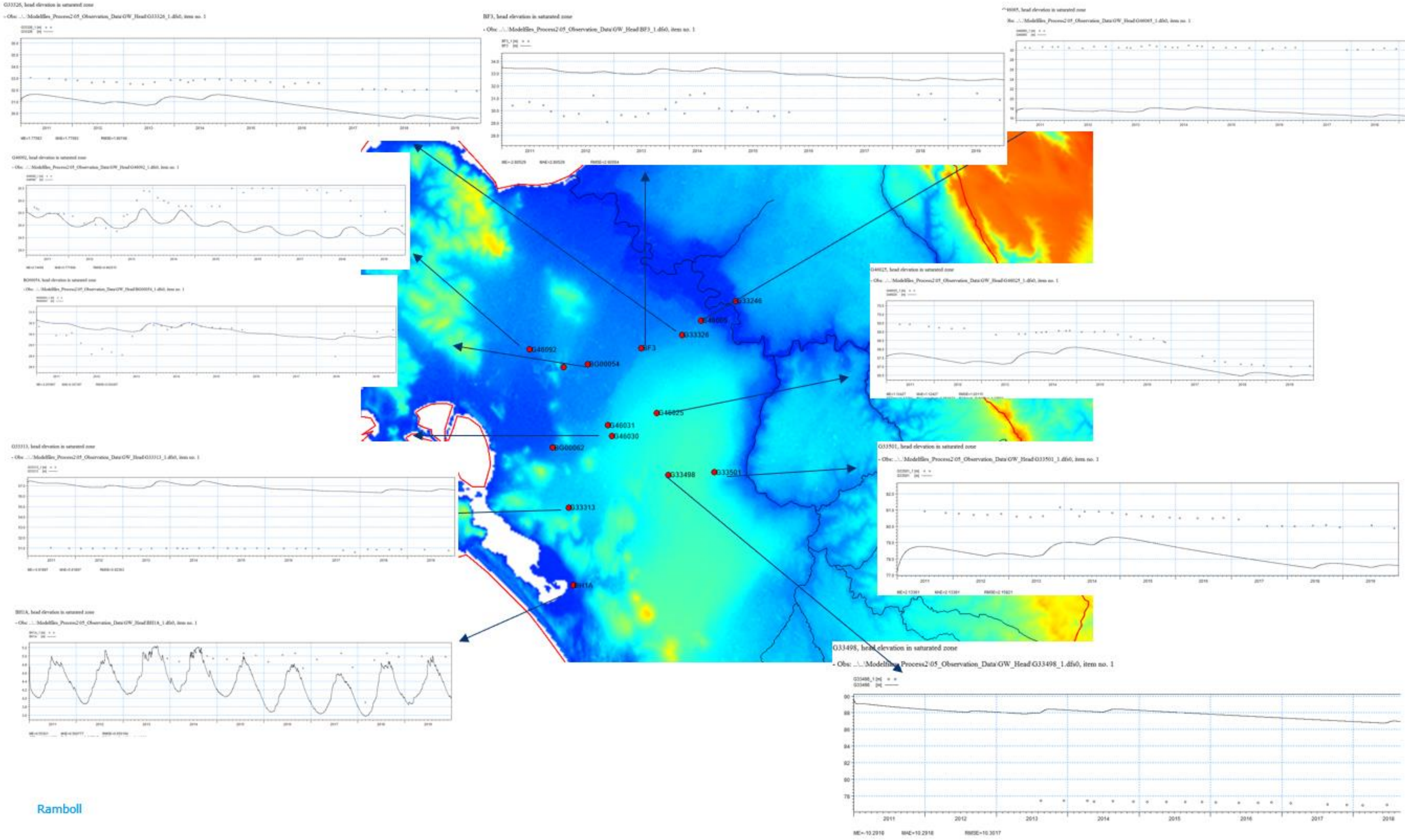

Figure 30 Simulated groundwater head in selected monitoring boreholes for the wellfield system

In Figure 31 the simulated discharge in Berg River at the estuary is shown and compared to the calculated inflow to the estuary, both from the Berg River (upstream) as well as from the surroundings (groundwater and overland flow). The contribution from the surroundings has been calculated as average on monthly basis /6/. There has not been defined any performance goal for the model's capability to simulate the river discharge. But as it can be seen there is an overall good agreement between simulated and calculated flow which is assessed to be satisfying at this stage.

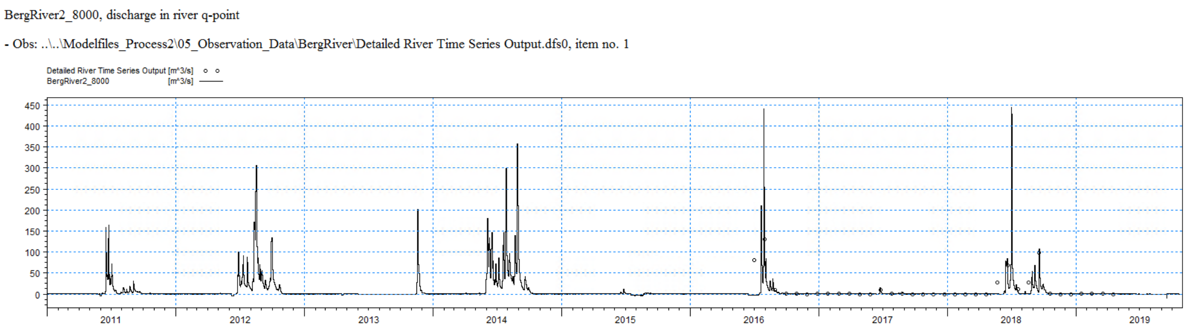

Figure 31 Simulated and calculated flow in Berg River at the estuary. The dots represent the calculated flow /6/

6. POTENTIAL HEAD MAP AND WATERBALANCES

The simulated potential head in layer 1 is shown in Figure 32. As it can be seen, the flow pattern in the upper aquifer is very much controlled by the topography with different flow directions within the area but with a dominant flow direction towards northwest.

In Figure 33 is shown the average water balance for the period 2015-2019. For this period the annual average rain is 325 mm and the simulated annual average recharge to the groundwater is only 6 mm leading to the severe droughts within this period. Furthermore, due to the drought, the storage in the aquifers have been reduced during the period. On annual basis the groundwater recharge has been negative in dry years as in 2017 shown in Figure 34.

In Figure 35 is shown the mean annual recharge to the groundwater for the calibration period. In general, the recharge to the groundwater is highest in more flat areas with alluvial deposits or sand dunes as around the wellfields. In this area the average annual recharge to the groundwater is 15-20 mm in the period 2015-2020. The groundwater recharge is generally lower in more elevated areas with surface near bedrock and steeper topography increasing overland flow. Around the rivers upward groundwater flow is general dominating.

On regional scale an average groundwater infiltration on 6 mm/year correspond to a groundwater resource on approximately 30 million m^3 in the model area. Only a part of this can be abstracted sustainably. Over-abstraction can for example cause poor water quality or unwanted impacts on wetland.

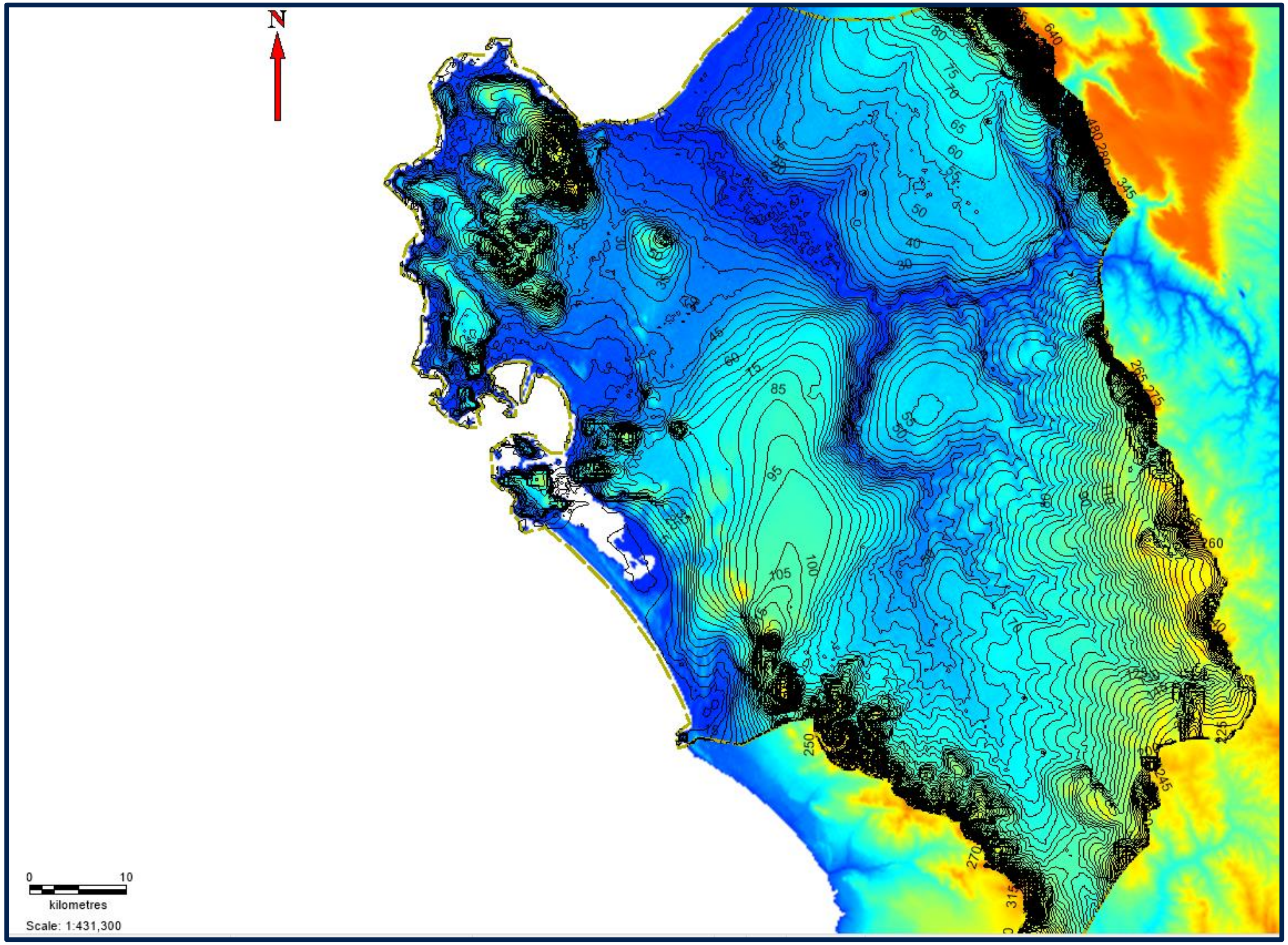

Figure 32 Simulated potential head map in the upper aquifer (average 2015-2020) in meters

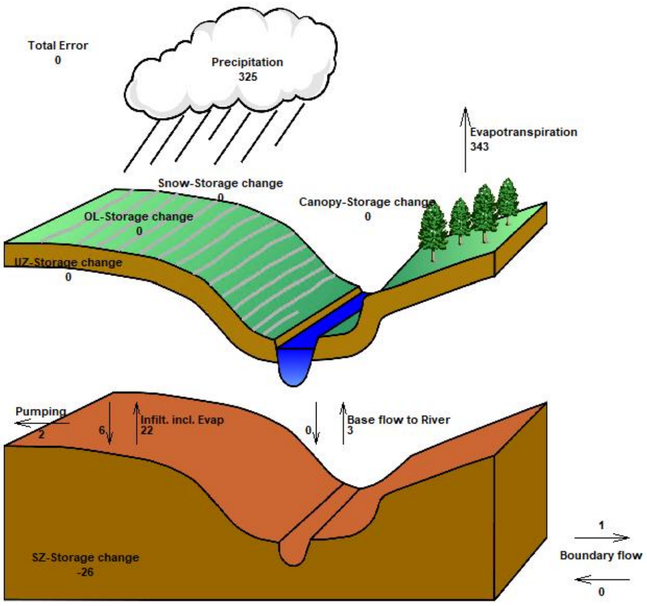

Figure 33 Average water balance for the period 2015-2020

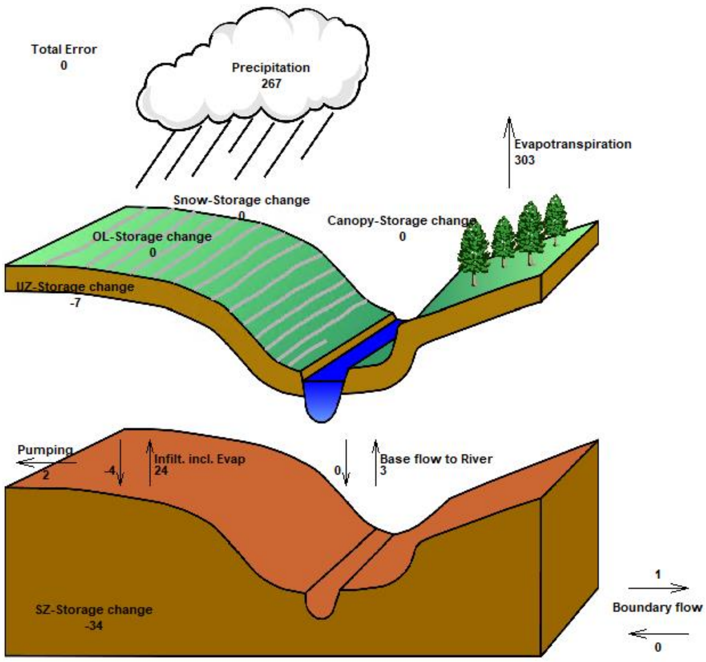

Figure 34 Water balance for 2017

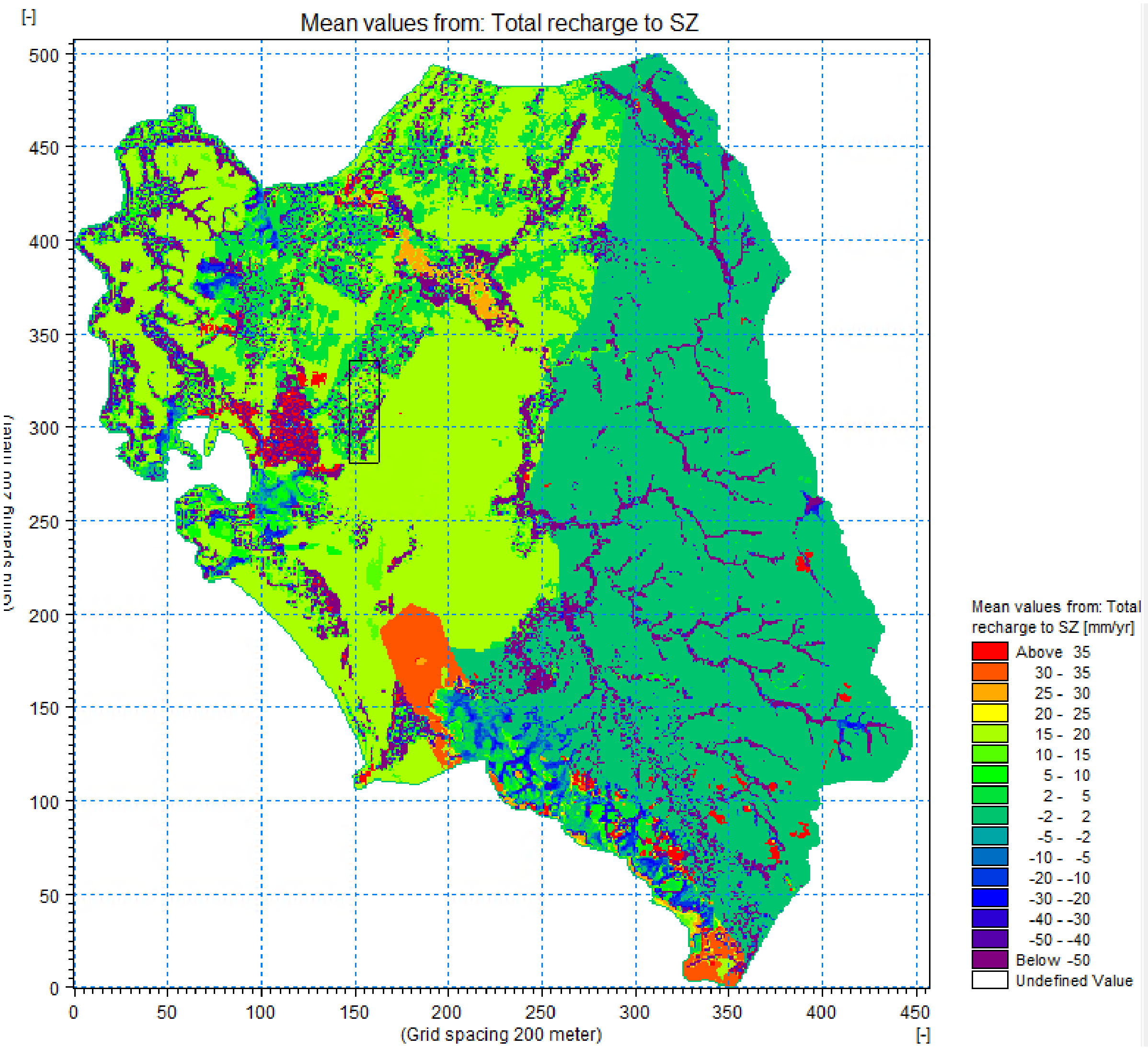

Figure 35 Mean annual recharge to the groundwater for the period 2015-2020

7. SCENARIOS

Five scenarios have been conducted following the calibration of the model. These are shown in Table 14. The scenarios have been run for the period 2005-2020. It was planned to run the scenarios for a longer period, but the quality of the data for potential evaporation prior to 2005 was questionable. Evaporation data before 2005 were measured mechanically and as it can be seen in Figure 36 this led to much higher evaporation rates, which is not estimated to be reliable, and for this reason the simulation period were shortened. Data for potential evaporation were collected from Agriculture Research council /10/.

Hopefield Wellfield has not yet been into operation, but abstraction and screens has been implemented according to information in /7/ and /8/.

Table 14 Abstraction rates in the 5 scenarios

Scenario		Total Abstraction (mill m3/year)	Abstraction Langebaan (mill m3/year)	Abstraction Hopefield (mill m3/year)
Scenario 1	Without pumping at all	0	0	0
Scenario 2	All abstraction from the Warm Database inclusive abstraction from Langebaan and Hopefield wellfields	11.4	2.92	1.6 /7//8/
Scenario 3	All abstraction from the Warm Database but without abstraction from Langebaan and Hopefield wellfields	6.9	0	0
Scenario 4	All abstraction from the Warm Database but without abstraction from Hopefield wellfield	9.82	2.92	0
Scenario 5	All abstraction from the Warm Database but without abstraction from Langebaan wellfield	8.5	0	1.6

The drawdown after 15 years when implementing the two well fields is shown on Figure 37. The cone of depression hasn't reached all the observation boreholes after 15 years. Even though the cone of depression hasn't reached important ecosystems as the lagoon after 15 years there will be simulated a flow reduction which can be implemented in WaterManager.

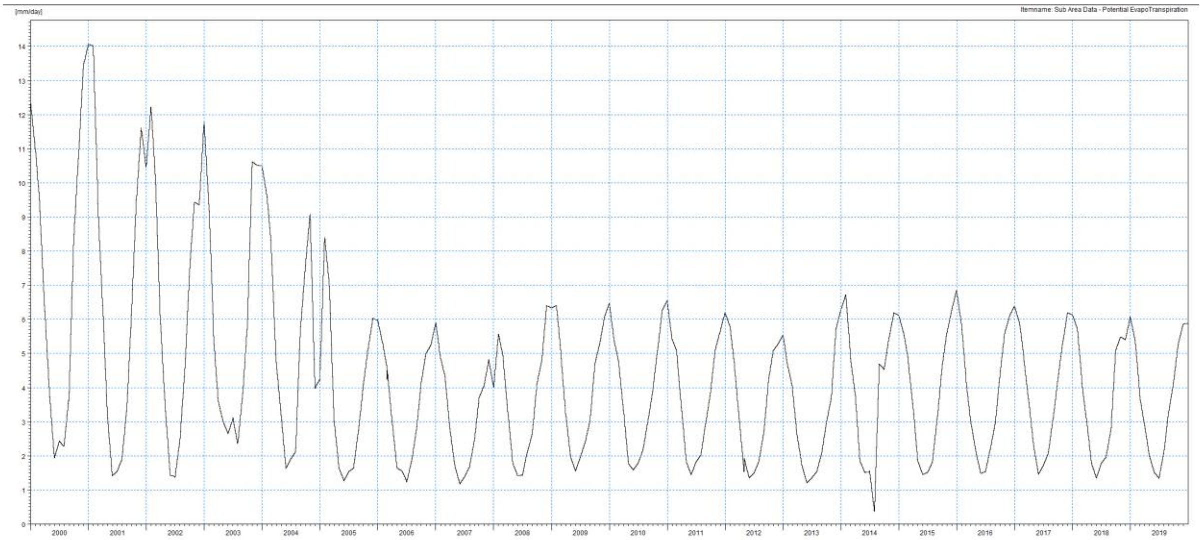

Figure 36 Data for potential evaporation /10/

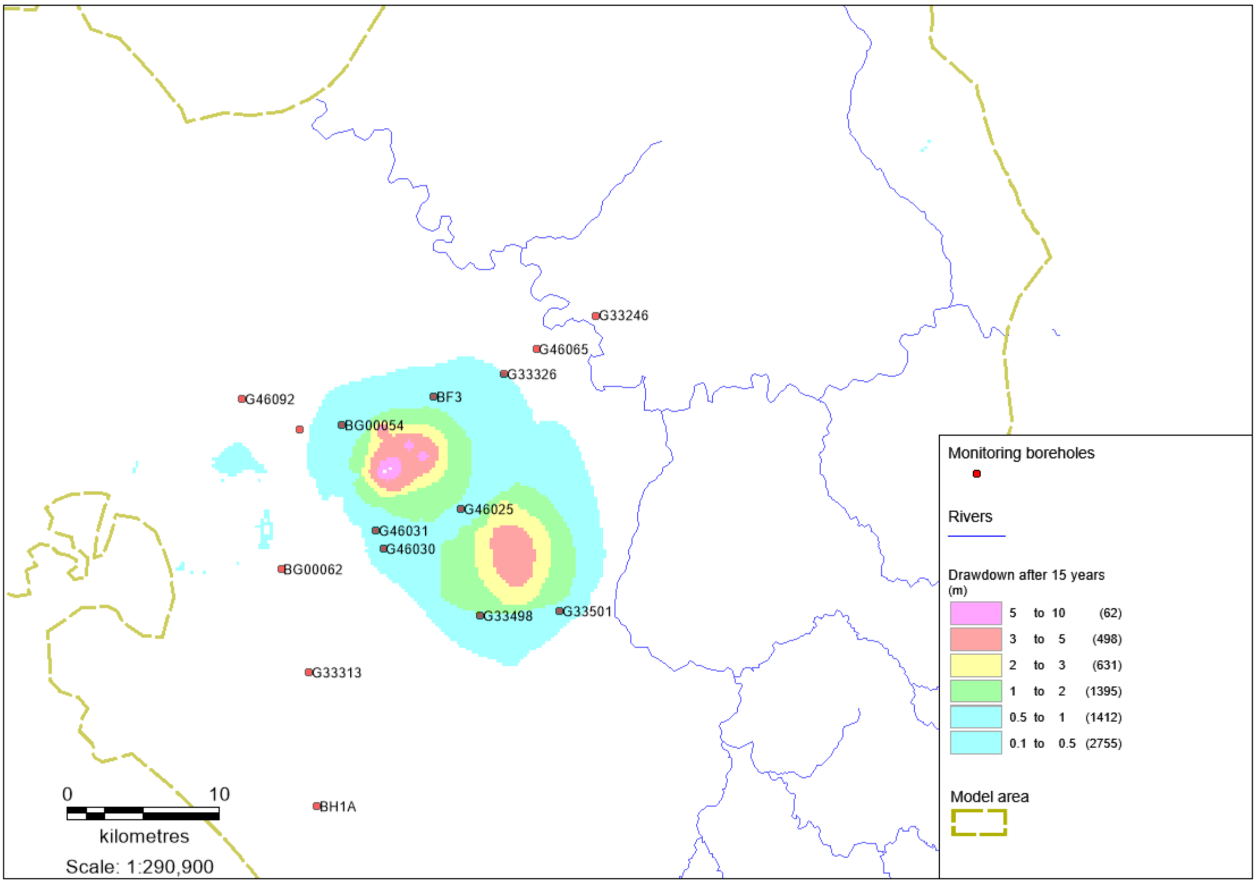

Figure 37 Drawdown in scenario 2 versus scenario after 15 years from start of pumping

8. DISCUSSION

The model is calibrated to conservative standard according to Danish criteria. This is in average for the model, but the model performance differs in the area, and is generally better around and north of Langebaan wellfield. The model is poorest south of Hopefield wellfield, probably related to a high geological heterogeneity in this area supported by a well-known fault system in this area. In general, the biggest uncertainties are estimated to be related to implementation of current abstraction rates and geological heterogeneities as faults. Moreover, the SKYTEM data have shown the occurrence of several clay layers separated by sandy layers in some areas. To describe this, the geological model must include more layers.

The model is interpreted to simulate the groundwater flow satisfying on aquifer level, but more precaution should be taken on borehole level. To get a model with higher accuracy, several improvements must be included, including a more detailed geological model, a more detailed study on the distribution of current abstraction rates on borehole level inclusive annual variations inn abstration and with inclusion of irrigation. To get a better match on simulated groundwater levels around Berg River, a fully dynamic solutions should be implemented instead of simpel routing. By doing this it is possible to include backwater from the sea related to the tidal water. These initiatives are recommended for the next model steps to improve the basis for the wellfield management system.

9. ACKNOWLEDGEMENT

A great acknowledgement to Nicolette Vermakk, Erika Braune, Julian Conrad,
David Wright and Johannes Van Der Werve for support of data and general support during the project.

10. REFERENCES

/1/ Danish Hydraulic Institute (DHI): MIKE SHE modeling system

/2/ South Africa SRMT 30 meters, updated 2018

/3/ Vermaak, Nicolette: Step-pump tests, from spreadsheet Weskus_Wish3

/4/ GEUS 2009: Good practice in hydrological modelling

/5/ Vermaak, Nicolette, 2021: Management strategies for the lower Berg Aquifer system, Western Cape.PhDThesis.

/6/ Zutari 2022: Flow measurements and flow calculations for Berg River

/7/ University of Western Cape 2019: Hopefield Wellfield: Geophysical Survey, Borehole Locations, Construction and Yields

/8/ Geoss 2019: Geohydrological input into a Strategic Environmental Assessment for the Greater Saldanha Area, Western Cape

/9/ DWS: Cross sections Berg river

/10/ Agriculture Research council 2022: Data for potential evaporation 1995-2020.

/11/ Saldanha Bay Wellfield model system (WFMS). Hydrostratigraphical model

/12/ Seylor, Helen, 2016: The Capture Principle Approach to Sustainable Groundwater Use